Efthymia Vakalopoulou, BSc

Ring opening metathesis polymerization derived polyHIPEs with novel features

MASTER'S THESIS

to achieve the university degree of

Diplom-Ingenieurin

Master's degree programme: Technical Chemistry

submitted to

Graz University of Technology

Supervisor

Assoc.Prof. Dipl.-Ing. Dr.techn., Christian Slugovc

Institute for Chemistry and Technology of Materials

Graz, September 2018

AFFIDAVIT

I declare that I have authored this thesis independently, that I have not used other than the declared sources/resources, and that I have explicitly indicated all material which has been quoted either literally or by content from the sources used. The text document uploaded to TUGRAZonline is identical to the present master‘s thesis.

Date

Signature

Στη γιαγιά μου Ευθυμία

και στον παππού μου Κωνσταντίνο.

Acknowledgement

Firstly, I would like to express my deep gratitude to Professor Christian Slugovc, who gave me the opportunity to work at his research group for completion of my diploma thesis. Also, I would like to thank him for his patient guidance and helpful advice both on this research work and on my future plans and decisions.

I also wish to thank various people for their contribution to my thesis; Professor Sergey Borisov for providing me the appropriate equipment and knowledge on the oxygen measurements, Professor Robert Saf for the SEM measurements and Mrs Josefine Hobisch for TGA measurements.

Furthermore, I would like to extend my thanks to people of my working group and colleagues in my office for the help and support during the diploma thesis.

Special thanks should be given to Onassis Foundation for the valuable financial support, which helped me to focus uninterrupted on my studies and successfully complete them.

Finally, I wish to thank my parents for their support and encouragement throughout my studies.

Abstract

Limitations referred to the swelling and deswelling behavior of dicyclopentadiene (DCPD) foams in unipolar solvents and hence to possible post-functionalization polymerizations, stimulated the formulation of foams of 80% nominal porosity from dicyclopentadiene (DCPD) and a second difunctional monomer bearing two polymerizable norbornene moieties. Surfactant stabilized high internal phase emulsions (HIPEs) with various monomer ratios were prepared and subsequently polymerized in order to obtain highly interconnected pore structures. The addition of the second monomer triggered the investigation of possible modifications on the morphology, the mechanical and thermal properties, as well as the swelling/deswelling behaviour in specific solvents. It will be shown that swelling and subsequent deswelling of monolithic foam specimens in solvents like toluene results in the same macroscopic structure of the monoliths as the untreated samples, facilitating post-polymerization functionalization. Additionally, the thermal properties reveal the influence of the second monomer on the crosslinking degree which directly affects the mechanical properties and the swelling-deswelling behaviour. In order to further enhance the research area of high internal phase emulsion templated polymer-foams, a different monomer, norbornadiene (NBD), was used to produce polyHIPEs. Although, NBD has structural similarities with DCPD and polymerizes via ROMP, the investigated properties were completely different from the respective DCPD based foams. Initially, emulsions of the monomer were prepared with three surfactants Pluronic L-121, P-123 and sorbitan monoolate (Span80) and their stability was examined under ambient and polymerization conditions. Following, they were cured and their morphology and mechanical properties were investigated and finally compared to the respective DCPD results from literature. Observation and IR measurements on the NBD foams show their ability to undergo fast oxidation under ambient conditions. The latter triggered the investigation of the behavior and rapidity, as well as the amount of oxygen the samples can consume under oxygen measurements taking place with atmospheric O_2 at ambient conditions.

Contents

1 Introduction

The ability to mimic the nature gives the opportunity to synthesize materials with special properties and features that can be used on numerous applications. Porous materials are an excellent representative example. As a pioneer, nature have already created many wonderful porous structures such as the honeycombs and bamboos.[1] Last 20 years, porous materials, and more particularly porous polymers continuously gain more and more interest, while articles referring to "porous polymers" significantly increased, leading to a modern trend.[2] Their popularity is mostly based on the high specific surface area and the well-defined porosity.[1,3] Also, their ability to form different kinds of porous materials such as monoliths, beads or films can broaden their application area.[1,2] As a new scientific object, the application range is satisfying and mostly focused on microelectronics, biomedical devices, membrane processes and catalysis.[2] In contrast to the number of applications, porous polymers can be prepared by following many strategies. The most common methods are the direct templating, the block copolymer self-assembly, the direct synthesis[1] and the use of colloidal systems such as emulsions, microemulsions, solid particles, or breath figure droplets.[2]

High internal phase emulsion or HIPE templating belongs to the colloidal system methods. The internal phase usually occupies more than 74% of the available volume and is the discontinuous phase, while the external phase is the continuous phase. The latter contains the necessary amount of monomer that under appropriate conditions can result the polymer network. Simultaneously, the elimination of the discontinuous phase leads to the creation of big and small voids and finally, to the formation of highly porous materials commonly called polyHIPEs. The voids can be either connected through windows rising on the thinnest parts of the polymer walls or they can be isolated closed-voids. Nevertheless, the type of voids and windows strongly depends on the type of the emulsion and the different ingredients. The conventional emulsions used for that purpose are water-in-oil (W/O) or oil-in-water (O/W) that cause the formation either of a hydrophilic or hydrophobic polymers, respectively. Apart from the internal and external phase, the preparation of stable emulsions requires the addition of an emulsifier, in that case a surfactant, which governs the interfacial tension between the two phases. Additionally, the conditions such as the temperature, the agitation and the nature of constituents, play important role on the preparation of the emulsion and hence on the polymer production. The polymerization is most commonly performed with radicals via free radical polymerization (FRP) and monomers like styrene,

acrylates and methacrylates. One of the most studied systems is the styrene polyHIPEs, but the poor mechanical properties, which exhibits, due to the low amount of crosslinking bonds, led to the addition of a second crosslinking monomer, the divinylbenzene. Although, the new styrene-*co*-divinylbenzene polyHIPE system was mechanically improved, the mechanical properties were not satisfied enough. For that reason, other polymerization techniques were investigated, including step-growth polymerization, atom transfer radical polymerization (ATRP), ring opening metathesis polymerization (ROMP)[1–4] and thiol−ene/yne click chemistry, which use several types of monomers and produce polymers with different properties.[3–5]

Dicyclopentadiene (DCPD) is a monomer that is polymerized via ROMP due to its high ring strain. It has been already extensively studied as a polyHIPE, which is formed though a stable W/O emulsion. The greatest advantage of DCPD is the existence of two double bonds. One double bond is used for the main chain production, while the second one connects the various polymer chains with each other, leading to a highly interconnected polymer network. As a result, the great crosslinking degree of the final polyHIPE produces quite stiff materials with outstanding mechanical properties compared to the styrene and styrene-*co*-divinylbenzene systems, without any further addition. The monoliths are characterized by the open-cell morphology and high porosity. Furthermore, they have the ability, according to the type of solvent, to swell by uptaking large amounts of solvents, and then to deswell. This property in combination to the free double bonds on the polymer chain can be used for post-functionalization reactions in solvents. Sometimes, though, upon deswelling the original porous structure is corrupted or even lost, narrowing the possible selection of solvents for post-polymerization functionalization. One type of functionalization that DCPD polyHIPEs exhibit due to the high degree of unsaturation is the reaction with the oxygen. The oxygen reacts with the radicals produced at the reactive double allylic positions, leading to the formation of various kinds of oxygen compounds such as hydroperoxides, alcohols, aldehydes, etc. The reaction undergoes both at elevated temperatures and ambient conditions and it is easily recognizable by the color change (white to yellow monoliths). Although, the DCPD polyHIPEs have been investigated in details, information about other monomers similar to DCPD that form polyHIPEs are few or any.[6–11]

Herein we initially report foams of nominal porosity of 80% formulated by DCPD and a second difunctional monomer bearing two polymerizable norbornene moieties, named crosslinking

comonomer (CLC). By adding the second monomer in different amount, we want to investigate how it influences the mechanical properties of the final polyHIPEs, as well as the behaviour under specific solvents. It will be shown that swelling and subsequent deswelling of monolithic foam specimens in solvents like toluene results in the same macroscopic structure of the monoliths as the untreated samples, facilitating post-polymerization functionalization. Accordingly, we report foams of nominal porosity of 80% synthesized by norbornadiene (NBD), a monomer structurally similar to DCPD, as it contains two double bonds and is polymerized via ROMP, but without the attached cyclopentadienyl group. We first present useful information about the stability of the NBD emulsions with different surfactants and subsequently, we study the morphology and mechanical properties of the respective NBD polyHIPEs. Finally, we investigate the oxidation behavior of NBD polyHIPEs under ambient conditions. More specifically, it will be shown that the polyHIPEs has the ability to rapidly remove large amount of oxygen from a well-defined container, with the possibility to cause anoxic conditions.

2 Theoretical Section

2.1 High internal phase emulsion (HIPE)

High Internal Phase Emulsion templating is a technique with increasing popularity and a satisfying area of applications. It belongs to a broader class called colloidal templating, which is suitable for producing macroporous microcellular polymers. All colloidal systems are based on the same principle. A biphasic system contains a polymerizable continuous phase and a removable discontinuous phase that is responsible for the pores creation.[3] In case of HIPE, the internal phase is the major phase as it occupies more than 74 % of the volume,[2–4] while the external is the minor phase and it contains the monomer. Depending on the polarity of the monomer, W/O and O/W emulsions can be prepared, leading to hydrophobic and hydrophilic polymers, respectively. The surfactant is the most important constituent for the HIPE formation because not only it renders the mixing of the two immiscible liquids but also ensures the stability of the emulsion. The emulsion preparation requires the dropwise addition of the major phase to a solution of the minor phase and the surfactant, under constant agitation[3] (Figure 1).

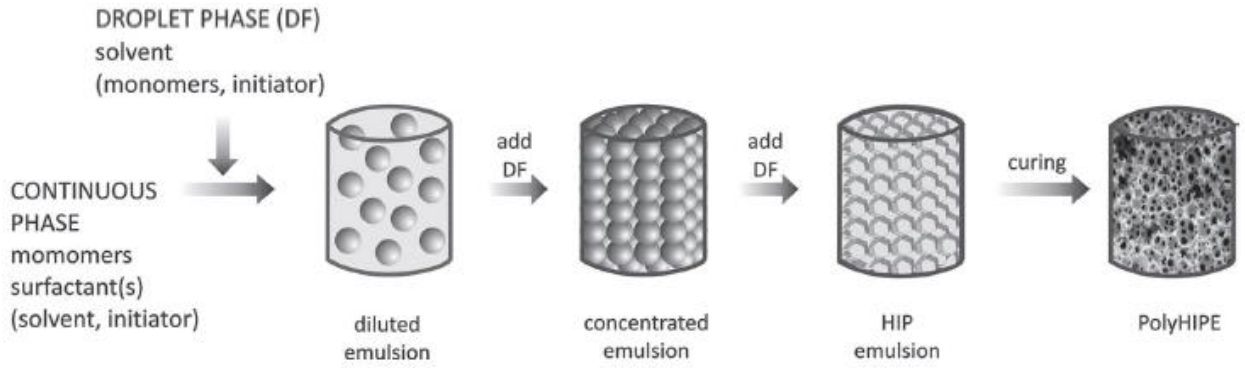

Figure 1.preparation of polymeric foams through high internal phase emulsion templating.[4]

A significant issue of HIPEs is the stability. Stability can be influenced from several factors, including the nature and the amount of the constituents, the temperature, the rate and time of agitation and the stabilizing salts. The increase of the viscosity can also influence the stability by hindering the coalescence. The continues stirring converts a polydisperse system to a monodisperse. However, at very high viscosities the agitation is difficult and consequently, less internal phase can be merged, leading to a polydisperse system. Also, rising temperature reduce the stability as it facilitates the coalescence. The nature of surfactant is also essential. The

surfactant must be soluble to the external phase in order to inhibit the emulsion destabilization or inversion.[3] Generally, a W/O HIPE requires a surfactant with low hydrophilic lipophilic balance (HLB)[3,4], while a O/W need one with high HLB.[4] In an emulsion, the surfactant lowers the interfacial tension between the phases. The higher the interfacial tension, the easier the surfactant forms a film between the two phases and finally results more stable emulsions. Last but not least, the addition of a salt boosts the film formation on the interface by lowering the surfactant-aqueous phase interactions and promotes the surfactant-surfactant interactions, resulting more stable emulsion. Additionally, salts impede Ostwald ripening, a process where the bigger droplets are selectively growing against smaller. As a result, aqueous phase becomes more insoluble in the oil phase leading to less attraction between the droplets.[3]

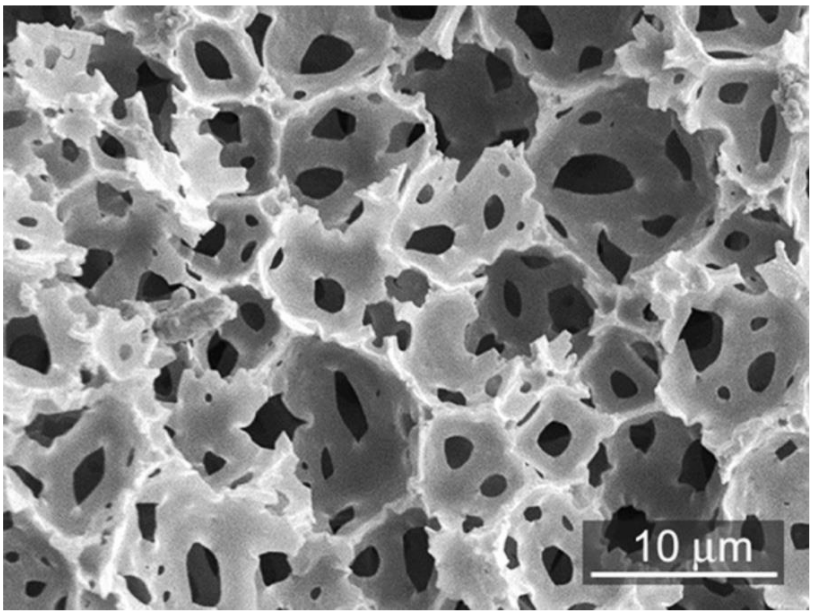

Figure 2.SEM picture of a typical open cell polyHIPE.[1]

A polyHIPE is synthesized when the external phase of a HIPE contains a monomer. The morphology between polyHIPEs and HIPEs is significantly different.[3] Voids and windows are two characteristic features of polyHIPEs (Figure 2). More specifically, windows are formed under certain condition at the thinnest parts of the continuous phase.[3,5] This situation transforms the discontinuous phase to a continuous network. The latter in combination to internal phase elimination results to open-cell polyHIPEs.[3] Moreover, the formation of open- or closed-cell polyHIPEs depends on the amount of the internal phase but mostly depends on the surfactant content.[3,5] Open-cell structure usually requires surfactant content above 7 % of the external phase,

while closed-cell polyHIPEs are formed with less than 4 %.[3] Generally, voids diameter is varied between 1 μm and 100 μm and it is strongly influenced by the stability of the emulsion. An increase in stability forces a decrease in the size of voids.[3,5] An interesting fact about polyHIPEs is the variety of shapes that can take, ranging from membranes to monoliths. More particularly, monoliths can be formed by molds of any shape and size. However, the mold's material is able to affect the surface morphology leading to either open- or closed-cell structure.[4]

According to studies, polyHIPEs are mostly synthesized via free radical polymerization (FRP) from W/O systems,[1–4] where oil phase contain the monomer and aqueous phase is the internal phase. Most investigated monomers are styrene, acrylates and methacrylates.[3] However, several other polymerization techniques can be adopted, including step-growth polymerization, atom transfer radical polymerization (ATRP), ring opening metathesis polymerization (ROMP)[1–4] and thiol−ene/yne click chemistry,[2] as well as different systems such as O/W, supercritical fluids for droplet phase and non-aqueous systems. These alternatives give the opportunity to overcome problems faced in FRP and to open new routes in research.[1–4]

A polyHIPE has medium surface area ranging from 3 to 20 m^2/g[3], although it was expected to be higher due to the network of interconnected voids[5]. The large size of voids[3,5] in combination with the bulk polymer walls diminish the surface area. Nevertheless, surface area can be considerably improved by using porogenic solvents[3] and high crosslinker amounts.[5] Besides surface area, polyHIPEs exhibit the typical stress-strain curve of foams.[3] Unfortunately, the mechanical properties are significantly poor.[5] A solution could be the increase of crosslinking bonds by incorporating a crosslinker such as divylbenzene[3] or by using bicyclo-monomers like dicyclopentadiene. The later type of monomers is polymerized via ROMP due to the high ring strain, resulting to a network without the need of an additional crosslinker.[4] Last but not least, a highly promising property is the ability to absorb liquids. The air within the voids is being replaced by the liquid, a tendency that is emanated by the interfacial tension between the polyHIPE and the liquid.[3]

Many applications of polyHIPEs have been already addressed in scientific literature and patents.[3] These applications are mostly based on the inherit properties of each polymer but sometimes the ability of post-functionalization can reveal new properties, increasing the applications possibilities.[1,3,5] Biomedicine and more generally synthesis field uses polyHIPEs as supports. A

characteristic biomedical example is the peptide synthesis on the solid material and generally the tissue engineering.[3,5] Also, biodegradable polyHIPEs fulfill the requirements for production of living scaffolds compared to conventional materials.[1] Separation, ion exchange, transportation of hazardous or flammable liquids and drug delivery are applications that based on the ability of the porous polymers to absorb liquids. Chromatography and sensing, also, take advantage of polyHIPEs properties.[3,5] Finally, polyHIPEs can be resulted to porous carbon monoliths via pyrolysis or be a template for inorganic monoliths.[3]

2.2 Dicyclopentadiene (DCPD) polyHIPEs

Last three decades, the research on porous polymers is gradually increasing, while polyHIPEs denote a huge jump the recent years.[1] However, as mentioned before a significant disadvantage of common polyHIPEs is the poor mechanical properties. An alternative and promising route to overcome that problem was the use of norbornene and norbornene-like monomers polymerized via ring opening metathesis polymerization (ROMP). Those monomers have noticeable ring strain that can lead to linear or crosslinked polymers via the olefin metathesis reaction. Additionally, there is a variety of norbornene-like monomers and norbornene derivatives polymerized through ROMP.[4] DCPD is a cheap by-product from steam cracking of naphtha and gas oil during the ethylene production.[4,6] The advantage of the DCPD monomer is that contains two double bonds, one is responsible for the polymer's main chain formation while the second forces the formation of crosslinking bonds between the chains. Although, a crosslinked network is synthesized by the double bonds, the degree of unsaturation is still considerably high. The latter provides the additional possibility for polymer post-functionalization (Figure 3).[6]

The polyHIPEs formed with DCPD show a typical open cell morphology with large voids and small interconnecting windows (Figure 3). It is prepared via a W/O emulsion where the internal phase is the water and the external phase the DCPD. The challenging step for the preparation of DCPD polyHIPEs is the emulsion stability. The emulsion must be kept stable as long as the polymerization occurs for preparing a rigid, tough and highly porous material. In order to avoid the phase separation, the polymerization must take place as fast as possible. Elevated temperature can speed up the curing procedure, but it has negative results on the emulsion stability. The key point on having a fast polymerization at high temperature without causing phase separation is the

use of a faster initiator. As a result, a fast initiator can give a DCPD polyHIPE with high porosity and much better mechanical properties compared to those prepared via FRP.[6]

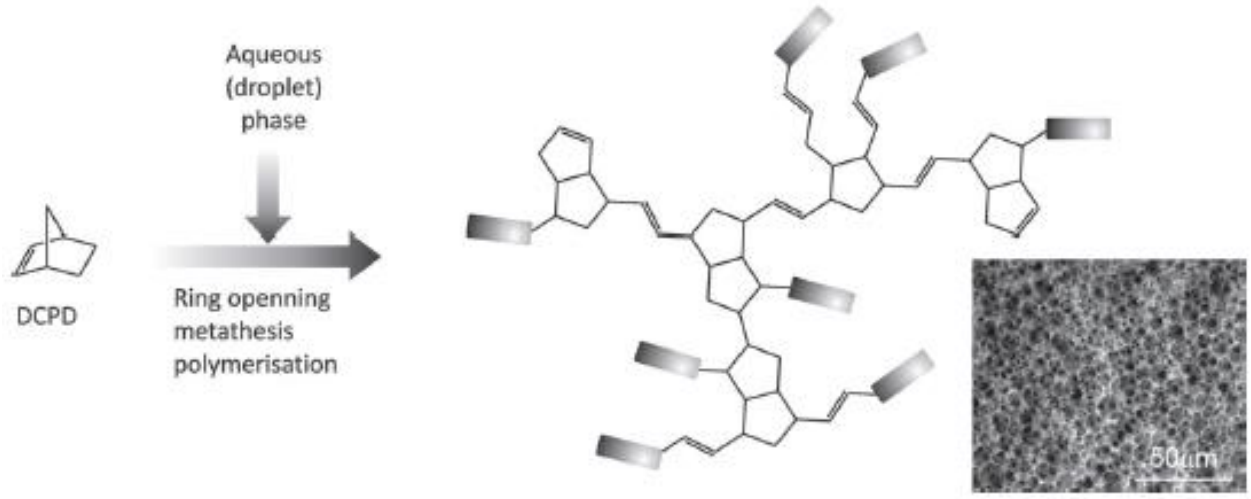

Figure 3. DCPD polyHIPE production via ROMP and its open cell morphology (SEM).[4]

Apart from emulsion stability, the mechanical properties are influenced by the amount of monomer or in other words the amount of the external phase. By varying the amount of external phase, many features such as porosity, windows and voids' size are being disturbed. For instance, low amount of monomer contributes in increasing the degree of porosity as well as the size of the voids and interconnected windows. The exact opposite results are observed in case of high external phase amount with a significantly high number of closed voids. Consequently, the different features affect the mechanical properties and more specifically, the rising amount of monomer lead to stiffer materials with noticeable plastic behavior.[7]

Another factor that influences the mechanical properties and morphology of the DCPD polyHIPE is the surfactant amount. Although, the different surfactant loadings affect insignificantly the porosity degree, the gradual decrease of the surfactant causes the formation of greater voids and windows' size on the monoliths. This phenomenon is attributed on the Ostwald ripening effect and the coalescence of the emulsion droplets. On the other hand, high surfactant amounts lead to more brittle and less plastic materials. In case of small amounts, the surfactant is mostly found in the interface between the internal and the external phase and it is easily extracted. On the contrary, at high surfactant loadings, an amount is concentrated within the polymer phase, resulting into

additional porosity and cracks during the extraction. The outcome is that the polymer walls collapse more easily upon a stress loading.[8]

The incorporation of another monomer polymerized via ROMP can influence many of the typical properties of a DCPD polyHIPE. For instance, the addition of the norbornene (NBE) (Figure 4) monomer in the DCPD polyHIPE show lower crosslinking degree due to the fact that the NBE do not contain the second double bond that is responsible for crosslinking. The morphology of the copolymer has the typical open cell morphology of the DCPD homopolymer, but with slightly larger voids, which cause a notable decrease on surface area. The mechanical properties illustrate variations due to the different amounts of the NBE but without following a specific trend. Last but not least, the thermal properties are influenced the most by the addition of the NBE. Particularly, the thermal stability and degradation rate are increased while the T_g is decreasing.[9]

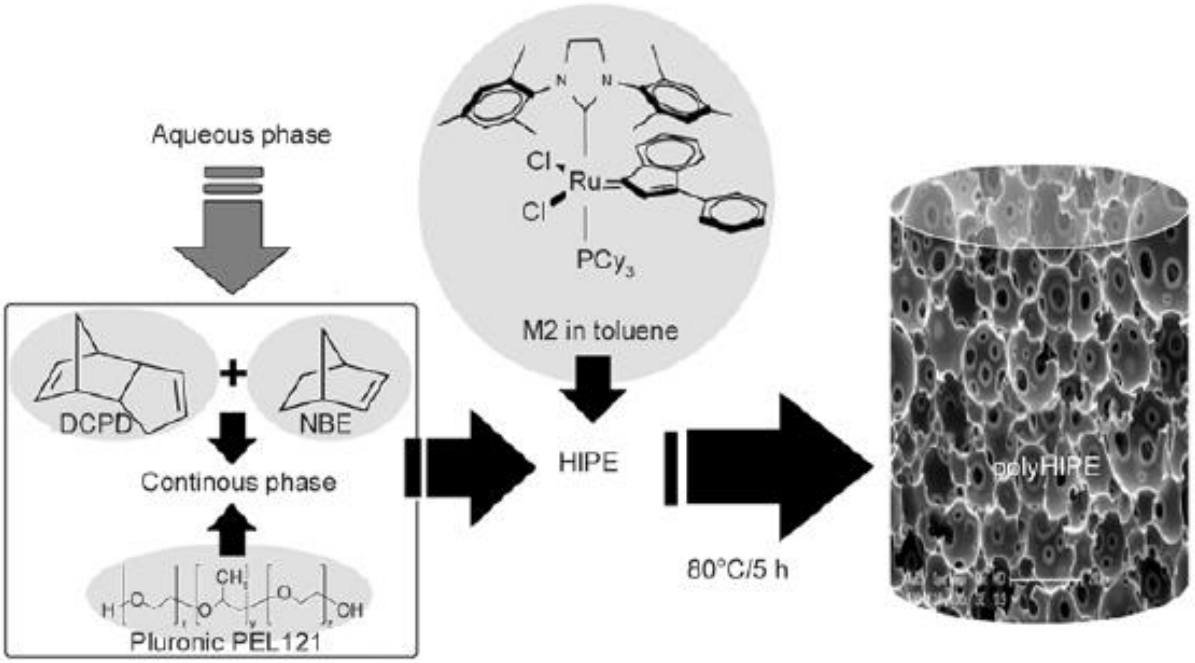

Figure 4. Production of DCPD-co-NBE polyHIPEs.[12]

A characteristic feature of DCPD polymer is the sensitivity to oxygen. Rather fast oxidation occurs when the polymer is exposed to air or water due to the high degree of unsaturation. On bulk polymers, the oxidation is more pronounced on the surface than in the inner parts, since the surface is directly in contact with the air. In case of DCPD polyHIPEs, the large number of voids and interconnected windows allow the air to diffuse through them, leading to faster oxidation of both

the surface and the interior area. A first indication for oxidation is the color change. White specimens are turn into yellow due to the formation of oxidation products such as carbonyls, hydroxyl groups, hydroperoxy groups and bridging peroxides.[7,10] The chemical observation of the oxidation is given by the elemental analysis (EA) and infrared spectroscopy (IR). The former provides an empirical formula of $C_5H_6O_2$,[6,10] while the latter illustrates one characteristic sharp peak at approximately 1700 cm^{-1} for carbonyl groups and one broad peak at approximately 3400 cm^{-1} for hydroxyl groups.[6] The oxidized monoliths exhibit different mechanical properties from unoxidized ones. They are brittle without considerable plastic deformation and maximum elongation hardly above 1%.[7,8] This particular behavior is attributed to the increase of crosslinking bonds within the polyHIPE either due to the covalent crosslinking between radicals or because of hydrogen bonding between hydroperoxides, carbonyls and hydroxyls.[10] Although unoxidized and oxidized monoliths show differences in mechanical properties, they do not reveal vital structural changes.[7]

An interesting ability of the DCPD polyHIPEs is the high solvent uptake. Apolar solvents such as THF and toluene can cause a significant uptake and swelling on monoliths compared to polar such as water both in unoxidized and oxidized samples. After a specific drying treatments, the structure and porosity of unoxidized materials can recover to some extent. This behavior indicates that capillary forces are acting during the swelling-deswelling procedure, which demonstrate remarkable mechanical features.[10] The ability of those monoliths to swell and deswell without losing their structure is useful for undergoing post-functionalization reactions. An example of post functionalization reaction with the DCPD polyHIPEs is the inverse electron demand Diels-Alder (iEDDA) reaction with tetrazines. An apolar solvent causes a pronounced swelling on the specimen in order to promote the penetration of the tetrazines and reaction with the double bonds in the porous structure. This reaction does not affect the polyHIPE morphology but lead to higher porosity.[11] The halogenation of the monoliths is also a typical example of post-functionalization reaction. Halogenated samples can be used as precursors for incorporating amines by nucleophilic substitution.[10] Thiol-ene reaction can be also undergone after the polyHIPE preparation by post-functionalizing a thiol bearing reagent. Generally, the high content of double bonds on DCPD polyHIPEs triggers the investigation for further functionalization. [6]

Apart from the common functionalization methods via solvents, DCPD polyHIPEs can be also functionalized via supercritical CO_2 ($scCO_2$). The latter is a promising alternative to replace the destructive and dangerous organic solvents. The functionalization via $scCO_2$ eliminates problems such as swelling and high temperatures, that faced in solvent functionalization. Additionally, the final materials are resulted directly after the process without further steps like filtration and drying. Last but not least, the monoliths remain unaffected during the procedure leading to functionalized open cell structure materials.[13]

The preparation of inorganic-organic hybrid porous materials is another way to change or to add new properties to the simply prepared foams (Figure 5). The procedure includes the addition of the inorganics such as nano-particles in the one of the two phases and afterwards the production of the polymeric foam. Generally, HIPE can be stabilized not only by using various surfactants but also by nano-particles or by the synergistic effect of the two alternatives. Those special emulsions are called Pickering emulsions. The particles are acting similar to the surfactant, as they accumulate in the interface of the two phases preventing their separation. Compared to surfactants, particles strongly affect the size, the shape and the surface energy of the emulsions resulting usually to closed cell polyHIPEs but they provide new properties such as conductivity and catalytic activity. On the other hand, the combination of both the particles and surfactant can lead to materials containing the advantages of both methods. A typical example is the nanocomposite foams prepared by DCPD and magnetic $\gamma Fe_2O_3/Fe_3O_4$ nanoparticles (FeO_x-NPs). The particular foams demonstrate open cell structure, noticeable mechanical properties[14,15] and high induction heating capability.[13] The preparation of macroporous ZnO foams is another example of using the Pickering method and divided into two steps. First, the emulsion is stabilized by the synergism of ZnO nanoparticles and surfactants. The second step is the calcination of the nanocomposite foam and finally the production of the inorganic foam. Generally, inorganic foams have many applications including filter systems, catalysts, absorbers, electrode materials.[16] A recent success in incorporating metal-organic frameworks (MOFs) nanoparticles in DCPD polyHIPE expanded the capabilities for synthesizing new materials with innovating properties. The specific hybrid foams are again a result of surfactants and nanoparticles combination leading to material with high porosity and a variety of applications.[17]

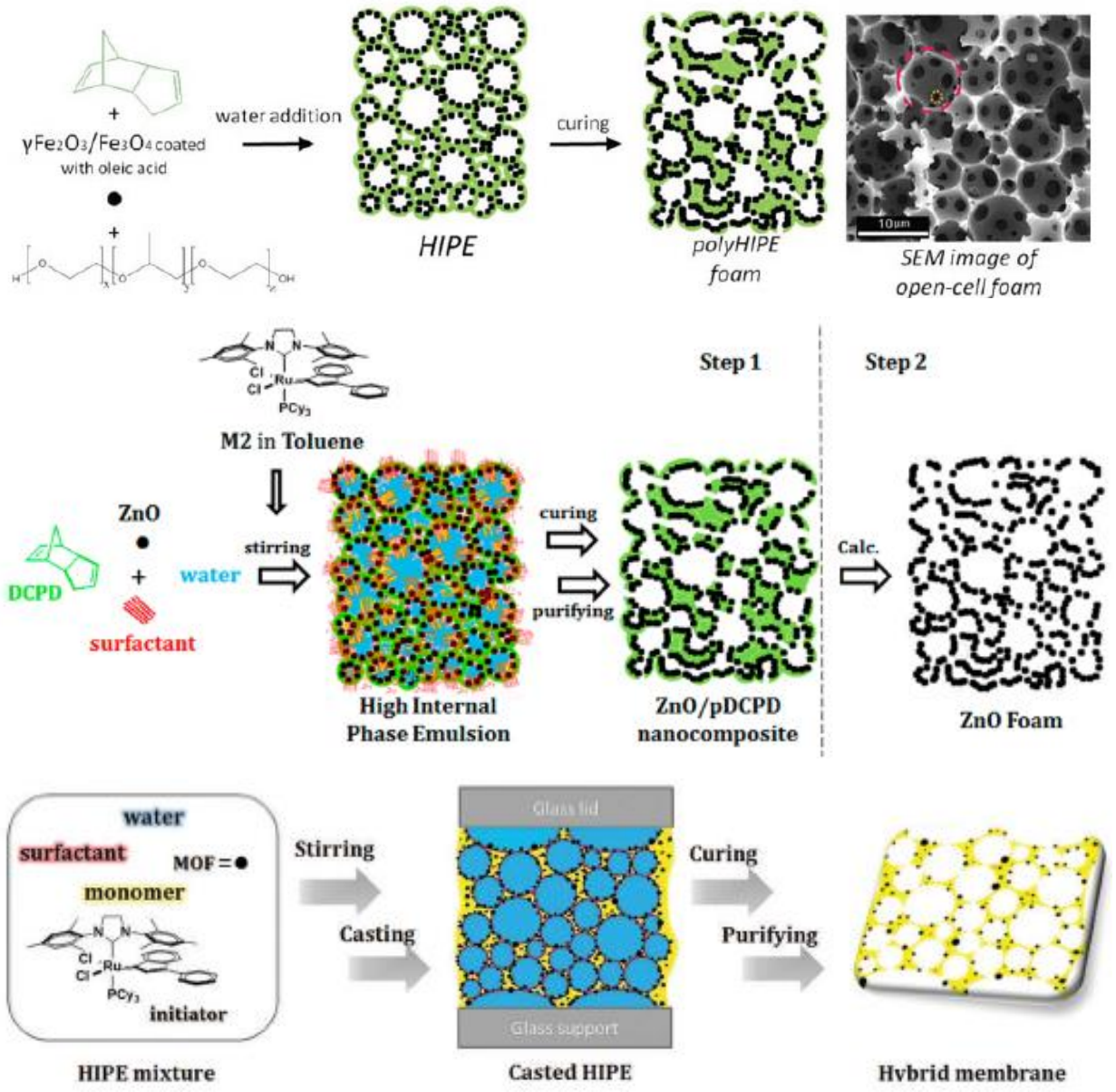

Figure 5. Preparation of inorganic-organic hybrid porous materials via Pickering emulsions, by using FeO_x nanoparticles (upper picture)[14], ZnO nanoparticles (middle picture)[16] and MOF nanoparticles (lower picture)[17].

The increased popularity for post-polymerization functionalization and the problematic recovery of the DCPD polyHIPEs after processes in solvents triggered us to investigate other routes which can possibly overcome such limitations. As a result, we formulated monolithic foams of 80% nominal porosity of DCPD and a second difunctional monomer bearing two polymerizable norbornene moieties, named crosslinking comonomer (CLC). The second monomer was expected to cause additional crosslinks as well as to provide more position for post-polymerization reactions. The additional crosslinks could change the mechanical properties and hence the

behaviour of the polyHIPEs in various solvents. Subsequently, we introduced the norbornadiene (NBD) monomer in HIPE templating technique. NBD is a monomer similar to DCPC as it bares two double bonds and polymerizes via ROMP. Although, the NBD has structural similarities with DCPD and forms successfully polyHIPEs, the investigated properties were different from the respective DCPD.

3 Results and Discussion

3.1 Chapter 1

3.1.1 Dicyclopentadiene (DCPD)/Crosslinking Comonomer (CLC)

For the current work, polyHIPEs were prepared by 20 wt% monomer mixture and 80 wt% water, while they were stabilized by a surfactant amount of 7 wt% according to the monomer mixture. The monomer mixture contained the well-known and extensively studied dicyclopentadiene (DCPD, Figure 6) and a second difunctional monomer bearing two polymerizable norbornene moieties named crosslinking comonomer (for study purposes, it will be referred to as CLC, Figure 6). Mixtures with different compositions were prepared in order to determine the influence of the increasing CLC amount on the defined DCPD properties. DCPD polyHIPEs (for experiment's purposes it will be referred to as P0) were also prepared for direct comparison with the newly composed polyHIPEs. The monomer mixture, which corresponded to the external phase, was placed in a flask with the appropriate amount of surfactant. Subsequently, the water, which corresponded to the internal phase, was added dropwise under agitation into the flask. The mixture was stirred for 1h after the water addition. As soon as the emulsion was ready a solution of the catalyst M2 in toluene was added and the HIPE was cured at 80 °C for 3h.

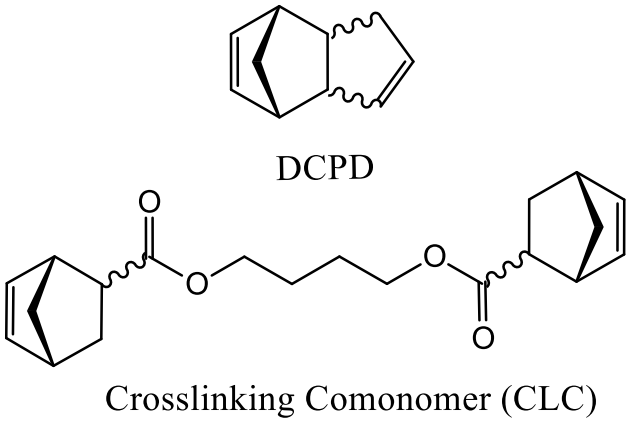

Figure 6. Molecular structure of DCPD (above) and CLC (below).

Before the foams production, it was necessary to examine the ability of the CLC itself to form stable HIPEs. The emulsion was seemed to be extremely unstable under ambient conditions leading to the need for investigation on HIPEs containing both DCPD and CLC. Tests showed that a 50-50 wt% monomer mixture is not capable to form stable HIPEs and thus the experiments were

always carried out with less than 50 wt% CLC. More specifically, four polyHIPEs with 10, 20, 30 and 40 wt% CLC were synthesized (for experiment's purposes they will be referred to as P10, P20, P30 and P40, respectively), characterized and compared.

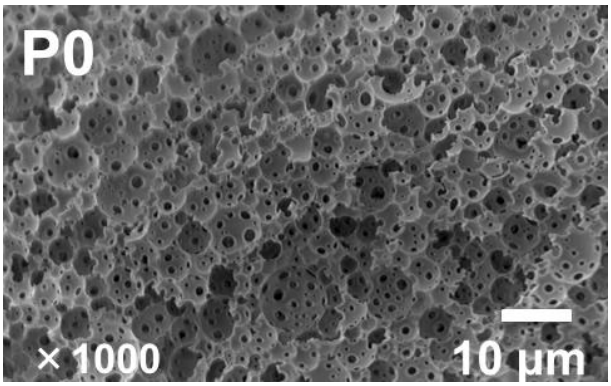

Figure 7. SEM picture of DCPD polyHIPE.

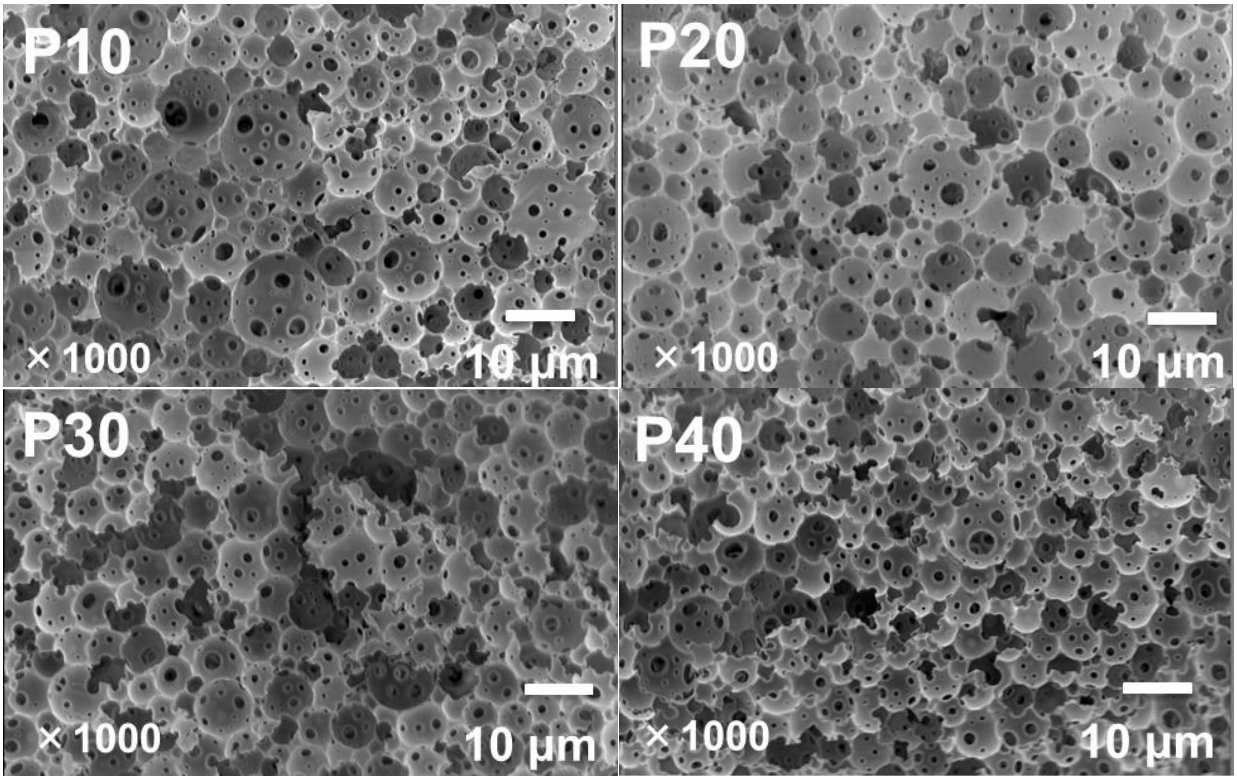

Figure 8. SEM pictures of DCPD/CLC polyHIPEs.

Initially, the morphology of the monoliths was investigated by SEM. The evaluation was done on the oxidized sample because they demonstrate high brittleness and there are no considerable differences on macrostructure.[7] SEM pictures (Figure 8) show that the new foams contain large voids and small interconnected windows referring to the common DCPD polyHIPE morphology

(Figure 7). This consequence indicates that the addition of the second monomer does not affect the open cell morphology of DCPD foams.

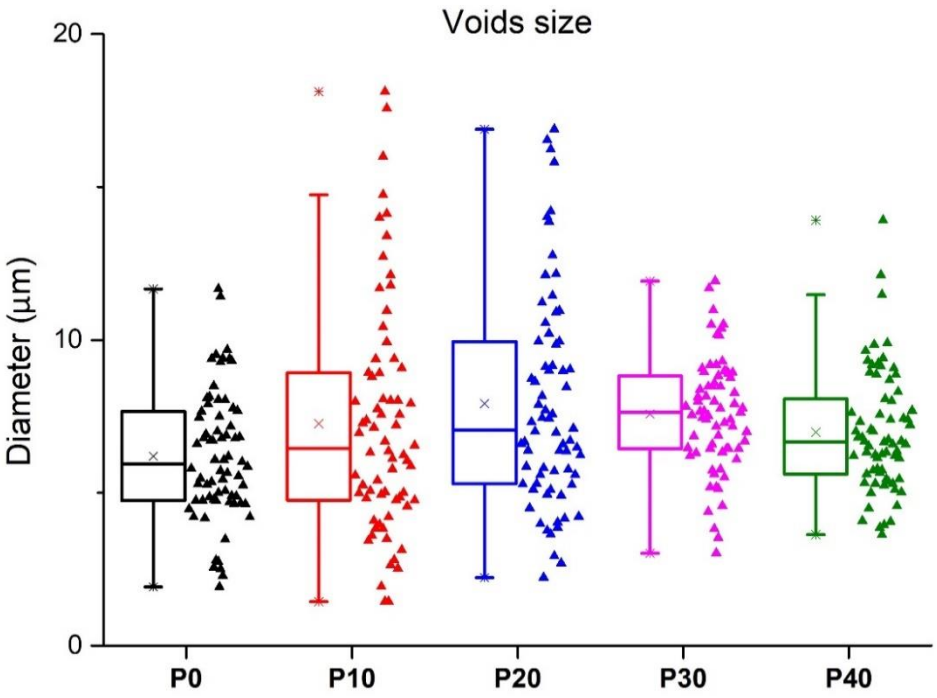

Figure 9. Box-whisker and beeswarm plots represent the data distribution referring to voids size of DCPD and DCPD/CLC polyHIPE samples.

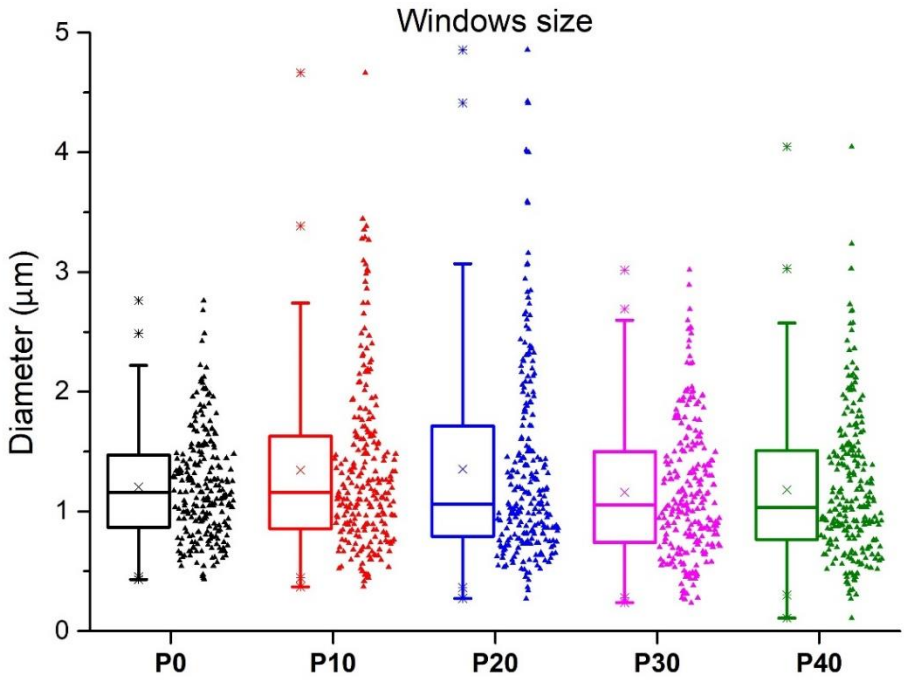

Figure 10. Box-whisker and beeswarm plots represent the data distribution referring to windows size of DCPD and DCPD/CLC polyHIPE samples.

Box-whisker plots in Figure 9 (whisker called the lines outspreading vertically from the boxes) illustrate the distribution of values referring to voids size of each sample. These plots are a beneficial tool for displaying in one graph the distribution of data belonging to different groups. Many information can be extracted by those graphs, such as the maximum and minimum values (in the edges of whisker lines or the individual spots above and below whisker lines), the median value (horizontal line in the box), as well as the average value (x-point in the box). Additionally, the distances between the horizontal lines in the graph (whisker and box edges) outline areas (known as quartiles) that contain equal amount of values. Long distances involve broadly distributed data, while short distances show narrow distribution. As a result, the boxes represent a restricted area where half of the overall values are included. On the right side of each box, there is a beeswarm plot showing a one-dimension dispersion of densely packed and non-overlapping data points. These plots together are able to provide a powerful description of the data distribution and hence more detailed information about the samples.

In case of voids diameter, the data show an increase both in value and distribution range up to sample P20 followed by a slight decrease. The same trend seems to be followed by the average value. A quite similar regime is also illustrated on the box-whisker plots of windows size (Figure 10). The calculation of the voids/windows (v/w) ratio from the average values revealed that the size ratio indicates only small fluctuations, so it can be considered as the constant value of 6. As a results, the combination of polyHIPEs features (voids and windows) do not affect the mechanical properties, instead the individual increase or decrease of their size can have a significant impact on mechanical properties. Generally, the voids and windows size can be partly responsible for the mechanical behavior of polyHIPEs. Large voids result stiffer materials while large windows lead to more brittle one.

There are two possible explanations for this outcome. The first explanation based on the stability of the emulsion by the CLC addition. From literature, it is known that the DCPD emulsions are characterized as stable at least under the curing conditions that also used at this specific work.[6] As mentioned in the beginning, CLC HIPE is not stable at room temperature, while the CLC/DCPD HIPEs with less than 50 wt% CLC are stable. However, the elevated temperatures used for polymerization are often destructive for the emulsions, forcing them to phase separation.[3] Thus, during curing procedure, the droplets can be aggregated in slightly larger one. The second and less

possible explanation implies that the SEM picture illustrates only a small area of the sample. However, we tried to provide pictures that are representative for the overall sample.

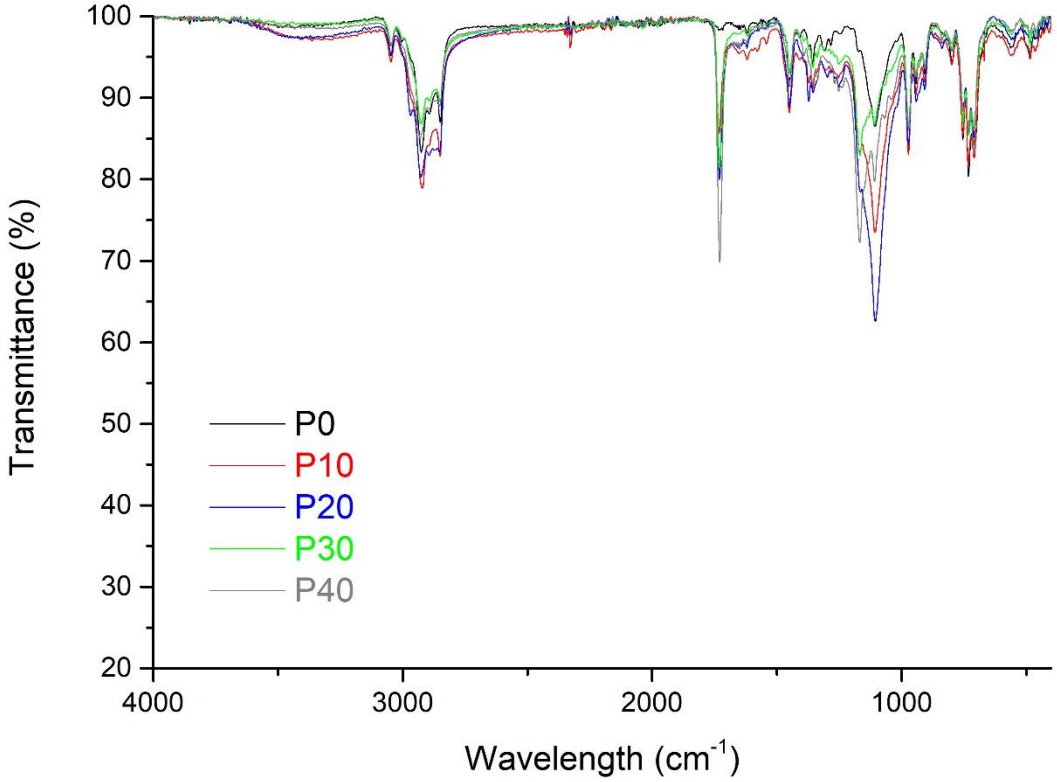

Figure 11. IR spectra of unoxidized DCPD and DCPD/CLC polyHIPE samples.

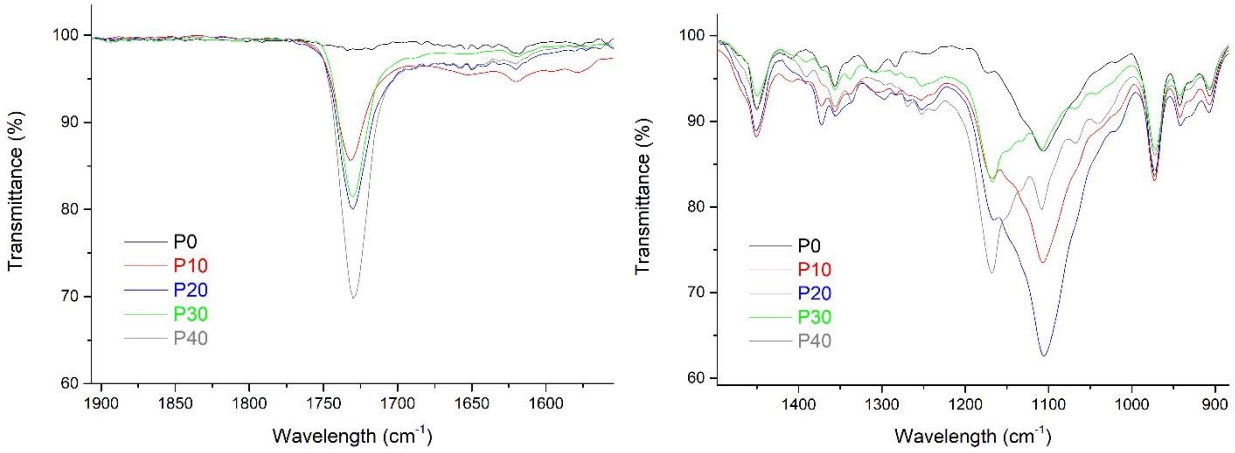

Figure 12. Magnified IR peaks at 1730 cm^{-1} (left) and 1100 cm^{-1} (right) of DCPD and DCPD/CLC polyHIPE samples.

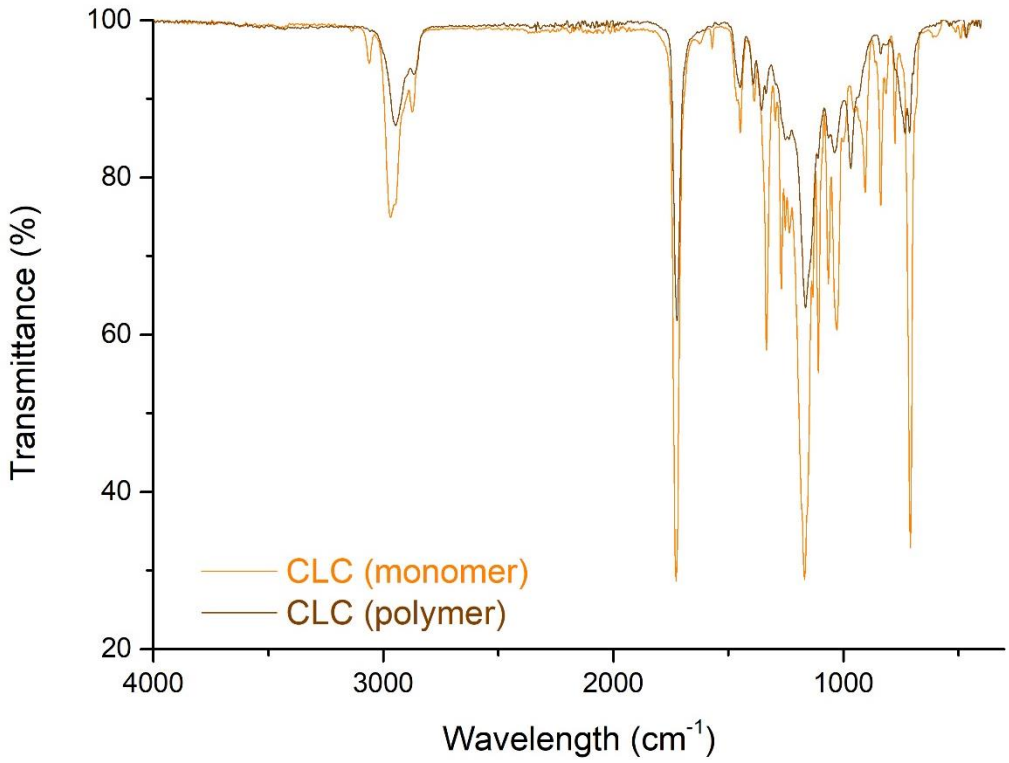

Figure 13. IR spectra of CLC monomer and bulk polymer

The next step was to identify the incorporation of CLC monomer on the copolymers. IR spectra were recorded on the unoxidized foams and bulk copolymers (for experiment's purposes they will be referred to as B0, B10, B20, B30 and B40). By comparing the spectra of P0, P10, P20, P30 and P40 (Figure 11), there are two peaks that differentiate among the samples, while the rest peaks such as at 970 cm^{-1} and 730 cm^{-1} that correspond to C = C trans and cis respectively, illustrate quite constant intensity. The peak at 1730 cm^{-1} is typical absorption for stretching vibration of C = O. CLC, as a norbornene ester compound, contains that specific IR peak both in monomer and bulk polymer with considerably high intensity. (Figure 13) The peak is also appeared at polyHIPE samples except for P0, while its intensity seems to increase with the increasing amount of CLC (Figure 12). The exact same peak and intensity trend was found in bulk copolymers (Figure A5). Such observations can provide a confident evidence for the copolymerization of DCPD and CLC. On the other hand, the peak at 1100 cm^{-1} (Figure 12) is appeared on every polyHIPE sample including P0 and corresponds to the C-O-C vibrations of surfactant L-121 (Figure A2). By comparing the IR spectra of polyHIPEs and bulk copolymers, it was clear that the peak was attributed to the remaining amount of surfactant in the samples (Figure A3), as it does not exist at

the IR spectra of bulk copolymers. Hence, it was not always able to completely remove the surfactant from the samples.

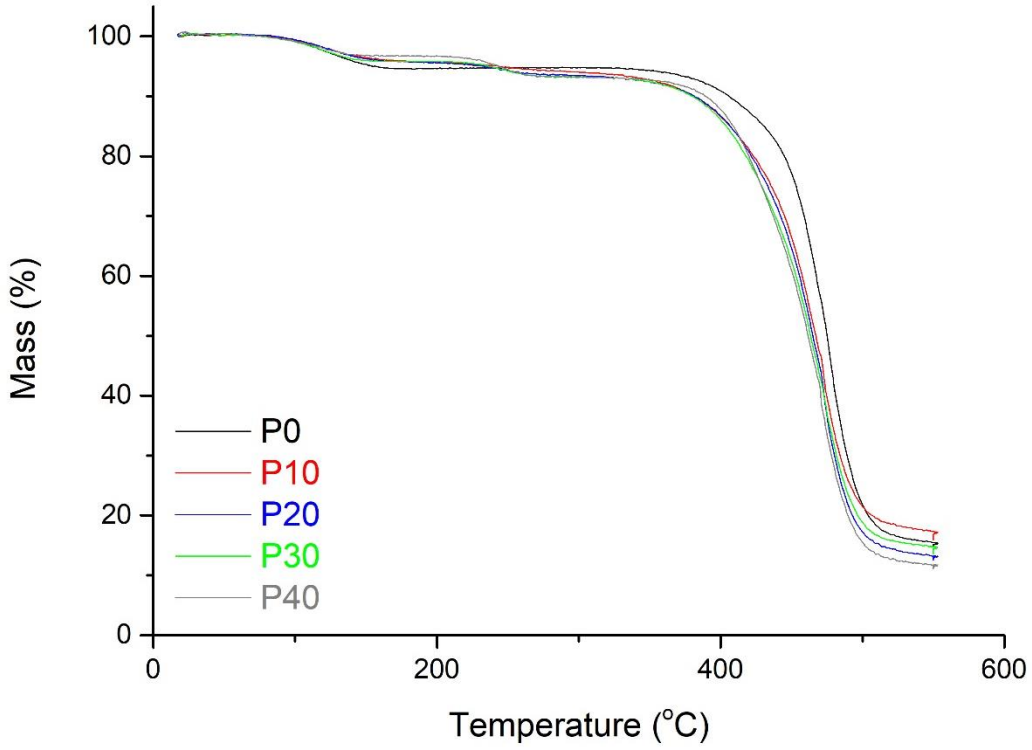

Figure 14. TGA curves of unoxidized dry DCPD and DCPD/CLC polyHIPE samples.

Thermal stability of polyHIPEs was investigated by thermal gravimetric analysis (TGA). Figure 14 represent TGA curves of the unoxidized and completely dry polyHIPE samples. By reading these curves, three separate mass losses can be distinguished. At temperature around 100 °C, there is a small mass loss. The comparison of TGA curves above and those referring to bulk copolymers (Figure A6) revealed that the latter do not display any mass change at the specific temperature range. The first assumption was based on the remaining amount of surfactant which was not used for the bulk copolymers preparation. However, the TGA curve of surfactant does not display any mass loss at 100 °C (Figure A7). Thus, we concluded with reservation that the mass change is possibly due to the loss of toluene. Small amount of toluene was added not only during the emulsion preparation but also for the bulk polymers production, in order to prevent the solidification of the DCPD. Although, both kind of materials cured under same exterior environment (80 °C), the interior conditions were considerably different. Polymerization is an exothermic reaction in both systems, leading to energy release which increases the temperature of

the surrounding environment. PolyHIPEs contain large amount of water that can absorb the released energy and compensate the temperature increase. Therefore, only an amount of water is possible to be lost under these conditions. On the other hand, production of bulk copolymers, which requires only the monomers and small amount of toluene, can cause the increase of sample's temperature and finally the loss of toluene during the polymerization.

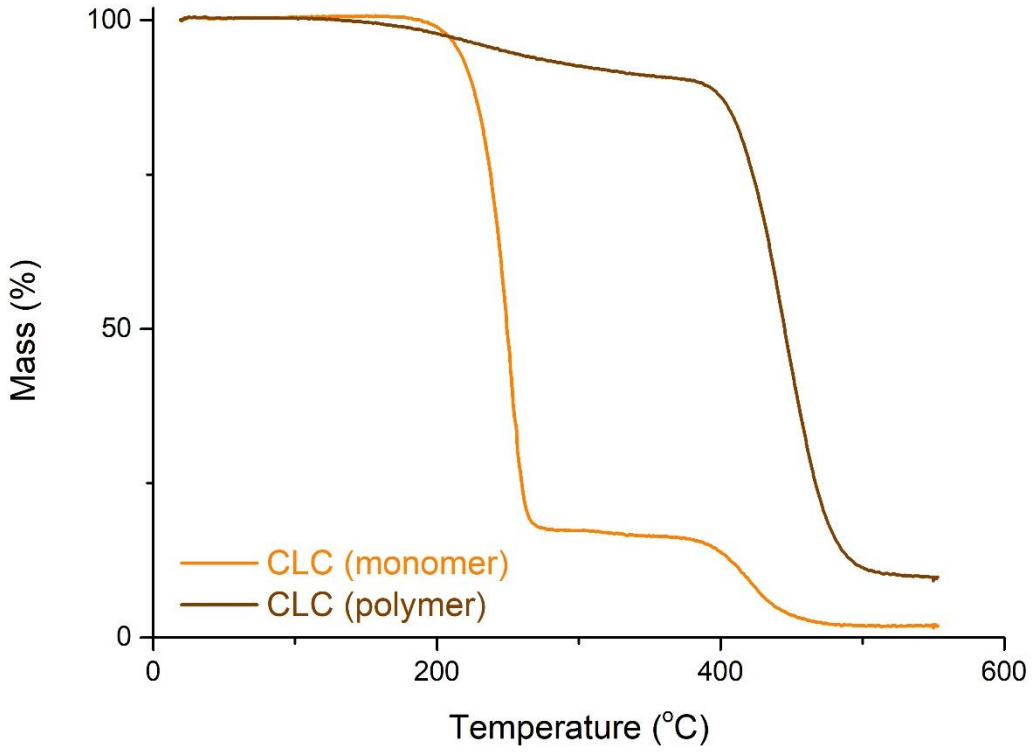

Figure 15. TGA curves of CLC monomer and bulk polymer.

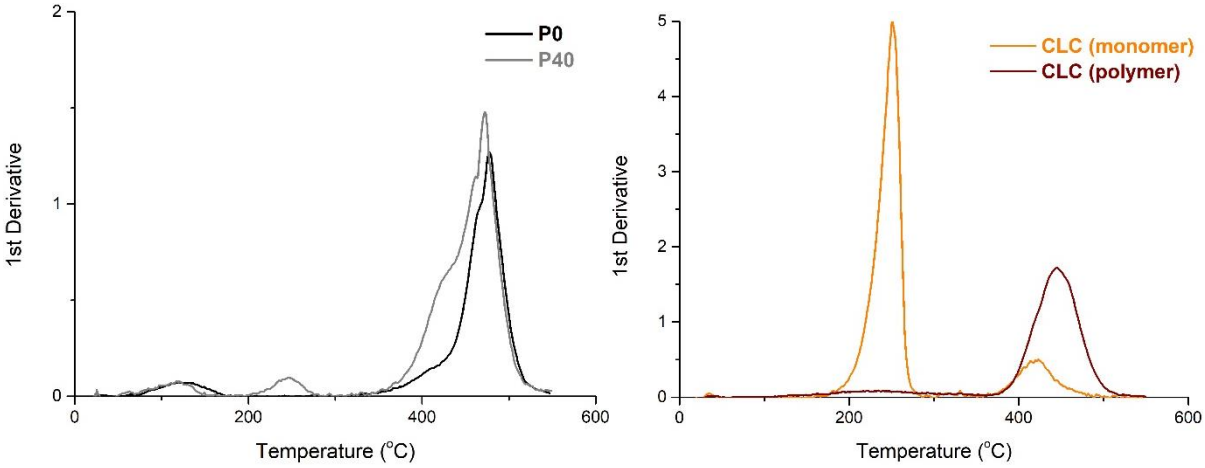

Figure 16. 1st derivative of P0 and P40 (left) and CLC monomer and polymer (right) TGA curves.

At temperatures around 240 °C (Figure 14), there is a second mass loss that occurs only on polyHIPEs and bulk polymers containing CLC, whereas DCPD homopolymer shows a plateau. This observation induced the analysis of CLC monomer and bulk polymer (Figure 15). Both of them show a mass loss at the same temperature range as our samples, but the CLC monomer has a considerably high mass change, leading to the outcome that the loss may be attributed to a reaction undergoing on free norbornene moieties. The mass loss is more clear on the 1st derivative of P0 and P40 and CLC monomer and polymer TGA curves shown in Figure 16. Retro-Diels-Alder is a typical reaction that occurs at temperatures higher than 150 °C on free norbornene and norbornene-based compounds. The existence of this mass loss on foams and bulk copolymers specifies that some of the CLC norbornene moieties are not crosslinked. Additionally, the loss percentage increases with the increasing amount of CLC. This information can be used to determine the free moieties fraction and therefore the crosslinking degree ascribed to CLC (CLC crosslinking degree) for every sample (Table 1). The percentage of the crosslinked norbornenes is found to be 71 % without serious variations, while by considering the amount of CLC used for every polyHIPE preparation, we end up to the conclusion that the CLC crosslinking degree gradually increases. Finally, if we assume that the crosslinking degree attributed to DCPD is not changing among the samples, then the CLC addition governs the overall crosslinking degree.

Table 1. Fraction of crosslinked norbornene moieties and crosslinking degree ascribed to CLC for DCPD/CLC polyHIPE samples

	Crosslinked moieties fraction (%)	***CLC crosslinking degree***
P10	72.4	7.2
P20	71.4	14.3
P30	72.0	21.6
P40	68.7	27.5

Finally, at approximately 390 °C (Figure 14), a large mass change occurs that is commonly appeared in polymers due to main chain degradation. This point is typical for identifying the thermal stability. P0 seems more thermally stable than the rest polyHIPEs, which degradation temperature is shifted slightly to lower temperatures. Nonetheless, we must be aware that P10,

P20, P30 and P40 have already undergone a mass loss prior to main chain decomposition, but still exhibit high thermal stability.

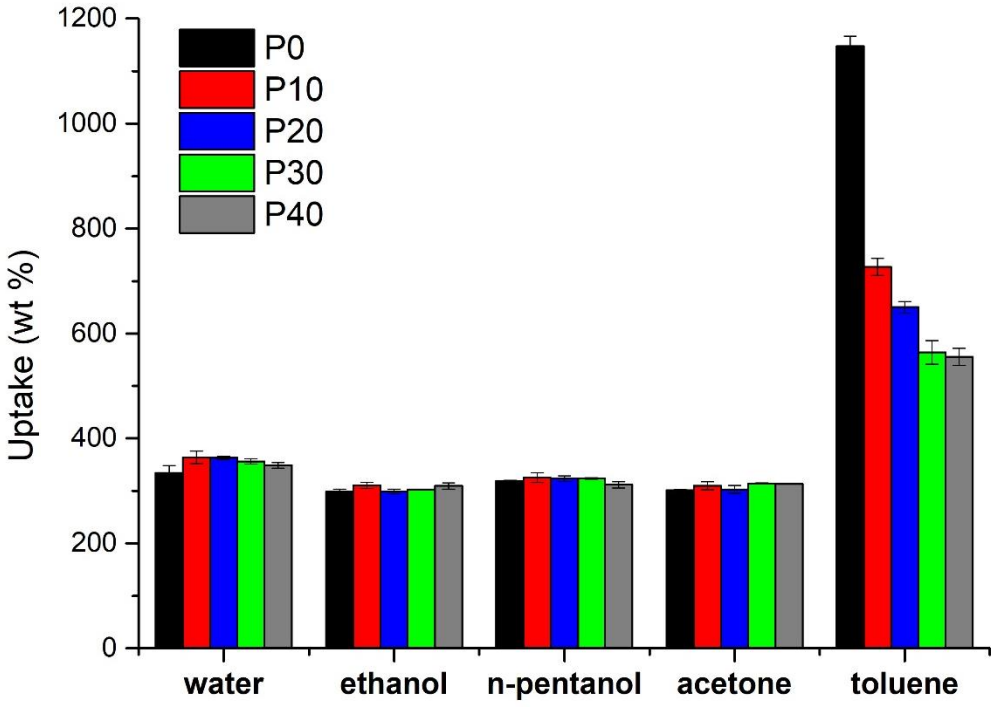

Figure 17. Solvent uptake wt% of DCPD and DCPD/CLC polyHIPE samples.

Thermal stability measurements were concluded that polyHIPE samples contain free norbornene moieties in different amounts and this can be utilized for possible post-functionalization reactions. Nevertheless, these reactions are usually taken place in solvents. Therefore, it was necessary to investigate the samples' behavior in different solvents. For this purpose, solvents exhibiting different relative polarities such as water, ethanol, *n*-pentanol, acetone and toluene were used. Figure 17 summarizes the solvent uptake of the different foams. In case of water, ethanol, *n*-pentanol and acetone, our polyHIPEs show a nearly constant uptake around 300 wt%, regardless the CLC amount. On the contrary, a huge toluene uptake is represented. More particularly, the rising amount of CLC causes lower uptake, which is still incredibly high. These results point out that the toluene uptake is accomplished both in foam's voids and polymer's walls, whereas the rest four solvents are accommodated only in the voids. The latter can provide useful information for the porosity of the foam and the relative density of the polymer.

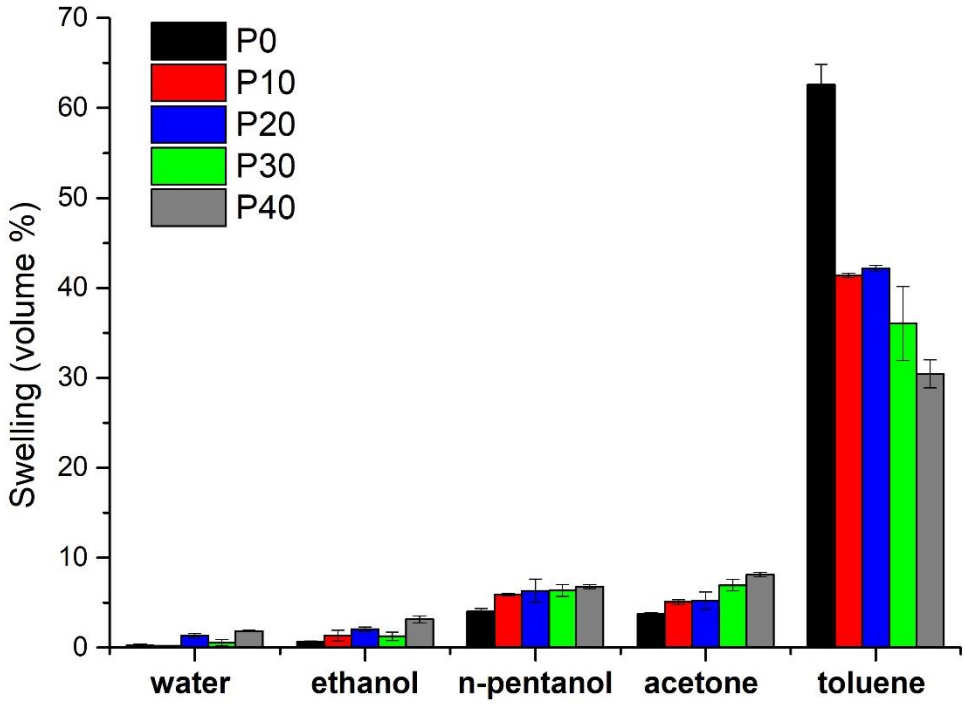

Figure 18. Swelling behavior of DCPD and DCPD/CLC polyHIPE samples under various solvents.

Simultaneous to solvent uptake, the samples reveal different swelling behavior under the solvent diversity. As it is illustrated on Figure 18, water and ethanol do not cause pronounced swelling, while acetone and *n*-pentanol affect the volume only to some extent. The fact that water and ethanol cause almost no volume increase and a roughly constant uptake by all foams, they were used for calculating the porosity of the foams and the density of the polymers. The calculations show porosity permanency among the samples, which perfectly matches with the initial hypothesis of preparing monoliths with 80 % porosity. The polymer density increases from 1.074 up to 1.095 g/mL with increasing amount of CLC.

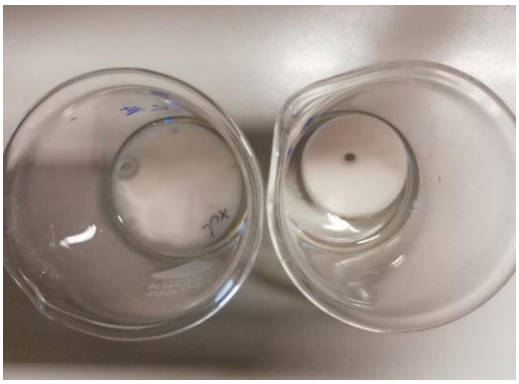

Figure 19. P0 (left) and P40 (right) during swelling procedure in toluene.

On the other hand, toluene triggers an increase in volume that follows the solvent uptake regime (Figure 18). This observation further confirms the TGA results referred to crosslinking bond ascribed to CLC. As mentioned before, if we presume that there is a constant DCPD crosslinking degree for all the samples, then the overall crosslinking degree changes only due to the different amount of CLC. Since the percentage of crosslinked norbornene moieties is constant, the rising amount of CLC increases the CLC crosslinking degree and hence the overall crosslinking degree of the samples. As a result, the foams become less and less flexible, exhibiting lower swelling effect and solvent uptake (Figure 19).

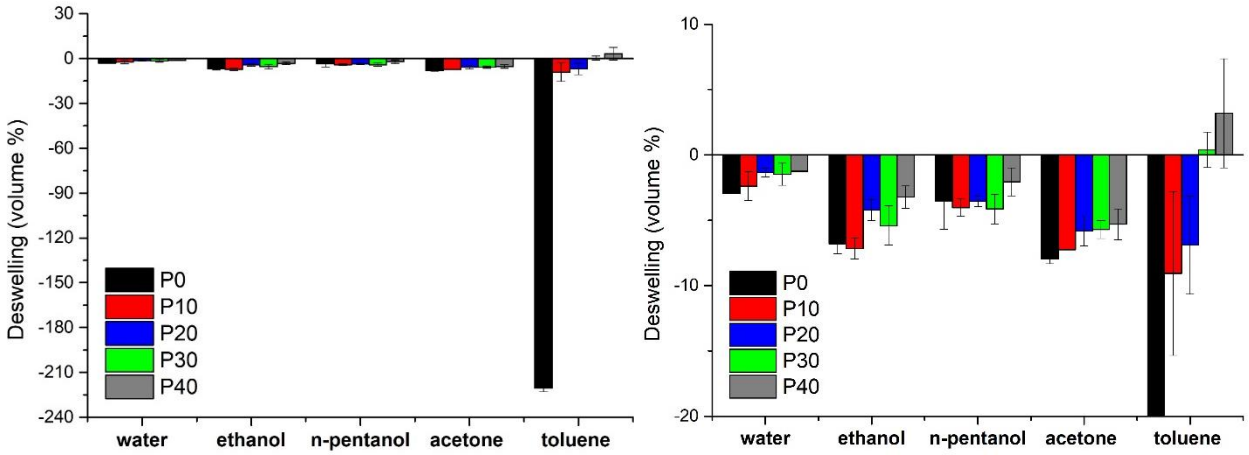

Figure 20. Deswelling behavior of DCPD and DCPD/CLC polyHIPE samples (whole range left, magnified in range -20 – 10 right).

The following step was to investigate the deswelling behavior of the polyHIPE samples. Considering all samples except for P0, the deswelling behavior follows a decreasing trend with CLC addition, but almost in all cases lead to shrinkage. The results referring to P0 are of great interest as it demonstrates shrinkage up to 230 volume% of its initial volume after swelling in toluene. The shrinkage is related to the collapse of the macroporous structure and hence, the P0 cannot be considered as polyHIPE anymore. In contrast, samples that contain high amount of CLC not only do not shrink but it is possible to remain slightly swollen (Figure 21). Consequently, the high CLC content on our polyHIPEs provides aside from the possibility for post-functionalization reactions on free norbornene moieties, the ability to recover their macroporous structure after reactions occurring in solvents due to the crosslinked norbornene moieties.

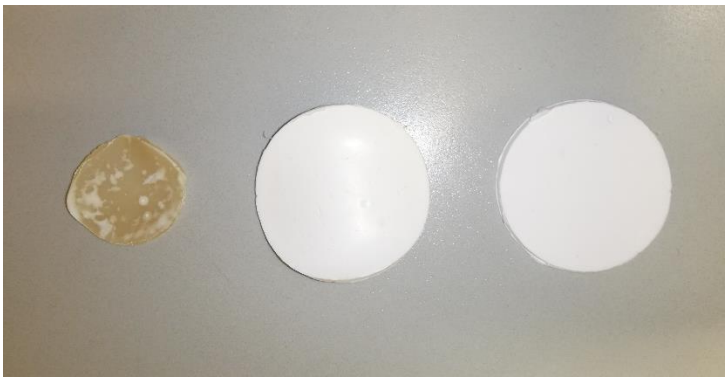

Figure 21. P0 (left) and P40 (middle) after swelling procedure in toluene and sample before swelling procedure in toluene (right).

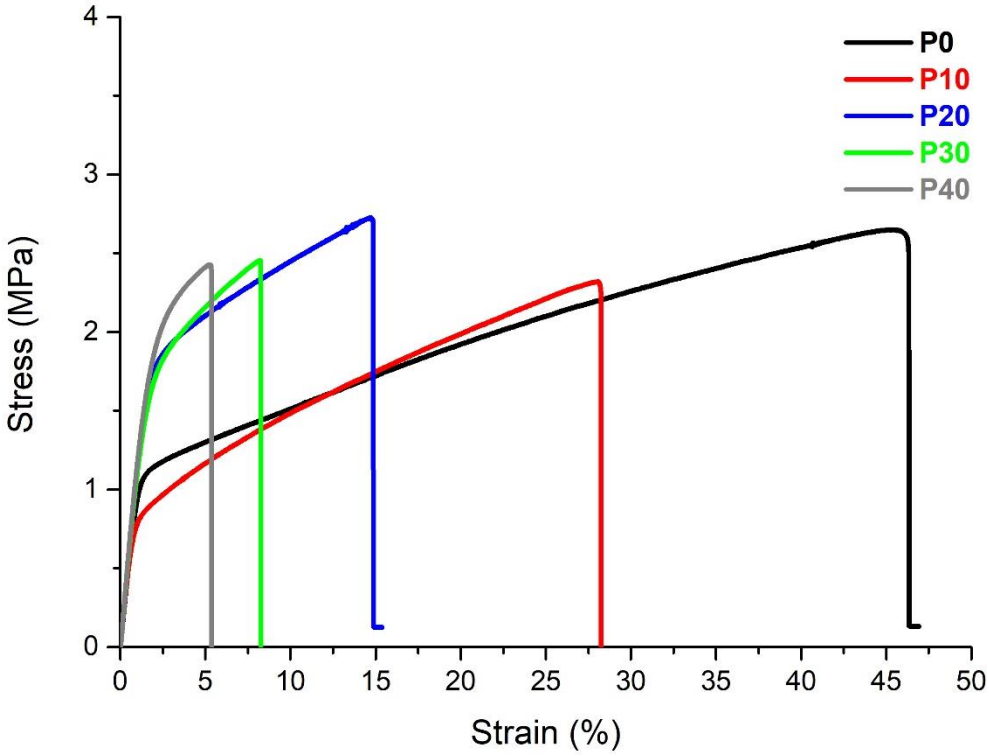

Figure 22. Curves resulted by tensile tests on unoxidized DCPD and DCPD/CLC polyHIPE samples.

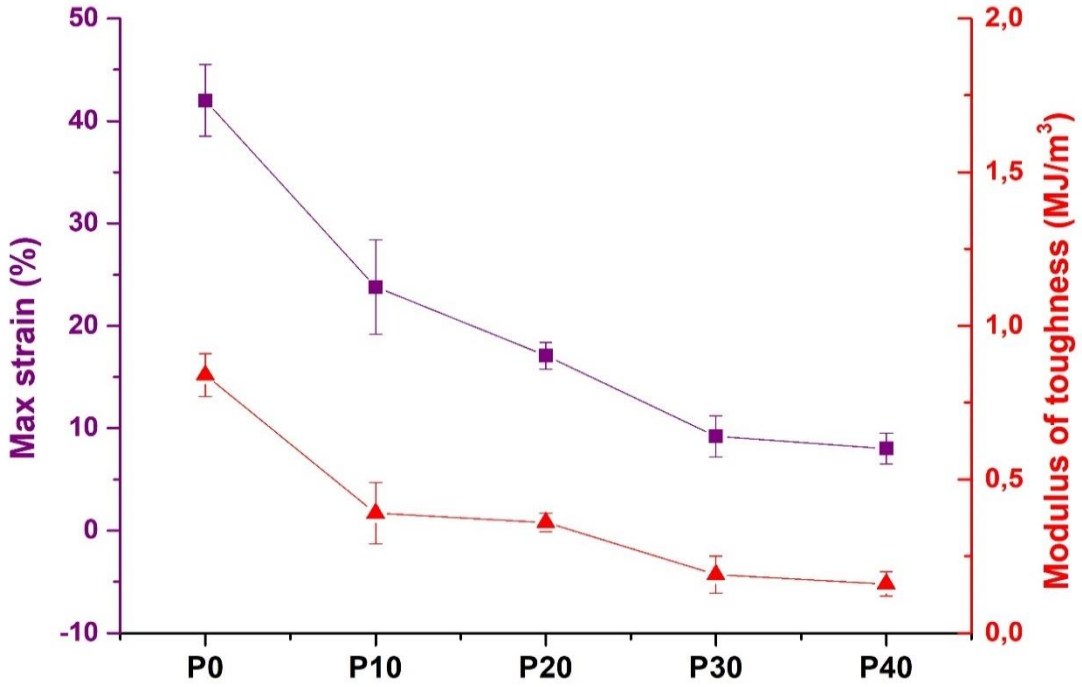

Figure 23. Decrease of maximum strain and modulus of toughness with increasing amount of CLC.

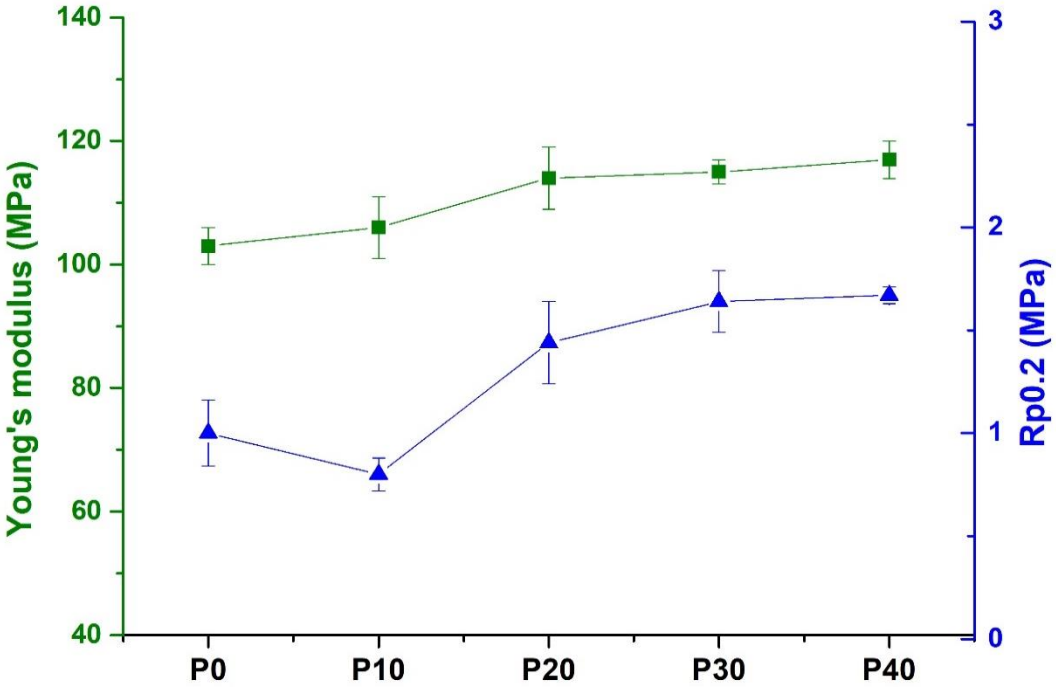

Figure 24. Increase of Young's modulus and yield point at 0.2 % strain with increasing amount of CLC.

Tensile tests were carried out on shouldered bars of polyHIPE samples, providing information about their mechanical behavior. Figure 22 illustrates the overall picture of the results. Some information can be directly extracted from the graph, such as the trend of maximum stress and

strain of the specimens. More specifically, the increase of CLC amount causes a gradual decrease on total elongation, while the stress applied ranges at the same values. Consequently, it can be directly concluded that the samples exhibit continuously lower toughness under a constant force (Figure 23).

On the other hand, the samples display steadily growing Young's modulus (Figure 24), where in case of P40 can reach values up to 117 MPa, one of the highest modulus resulted for unoxidized polyHIPEs. This means that the stiffness is higher on polyHIPEs containing more CLC. The above is perfectly reflected to the high CLC crosslinking degree resulted by TGA measurements, as well as to the reduced swelling effect on samples with high CLC amount ensued by swelling observations. Nonetheless, we have to consider that the samples are not bulk materials, instead they enclose a significant number of voids and windows, which as referred in the beginning can greatly influence the mechanical properties. Additionally, even if we were not able to determine the amount of crosslinking bonds derived by the DCPD, we have to mention that they have a great impact on the mechanical behavior, especially if its amount varies among the samples. Last but not least, the offset yield point at 0.2 % strain follows the Young's modulus regime. The samples with higher amount of CLC require higher forces to reach the same degree of elongation. The latter is in accordance with the swelling and deswelling behavior, where both P40 and P0 were subjected to same forces in the toluene solvent, but the former was swollen to some extent and then returned to its initial shape, while P0 was swollen and then entirely loss the macroporous structure. Finally, it must be mentioned that the greater increases and decreases are noted between either P0 and P10 or P10 and P20, because P10 represents an intermediate situation due to the low CLC content, and hence it can behave either as the DCPD homopolymer or as the copolymers.

3.1.2 Conclusion 1

In the current work, we presented HIPE preparations consisting of DCPD and a second difunctional monomer bearing two polymerizable norbornene moieties, CLC, in various compositions, a non-ionic surfactant and water. Subsequently, the HIPEs resulted via ROMP into foams of 80% nominal porosity. The addition of the comonomer did not change significantly the morphology of the polyHIPEs. Thermal analysis showed a decrease in the thermal stability of the foams with higher CLC amount. However, the most important outcome from this measurement was the determination of the crosslinking degree referring to CLC. The increasing amount of CLC

induced a great increase on the CLC crosslinking degree. On the same time, a moieties fraction of approximately 30% remained free and available for post-functionalization reactions. Additionally, the monoliths exhibited different swelling-deswelling behavior in various solvents depending on their CLC amount. More specifically, swelling and subsequent deswelling of the specimens with increasing CLC amount in toluene demonstrated no changes on their macroscopic structure, facilitating possible post-polymerization functionalization. Finally, mechanical properties were resulted by tensile tests on samples and revealed that the foams are getting stiffer exhibiting increasing E-moduli from 106-117 MPa, but also less tough with values from 0.84-0.16 MJ/m^3.

3.2 Chapter 2

3.2.1 Norbornadiene (NBD)

Norbornadiene (NBD) is a bicyclic compound with a significant ring strain that allows the polymerization via ring opening metathesis reactions. The existence of two double bonds on its structure forwards not only the polymerization but also the crosslinks among the chains, leading to highly insoluble polymeric networks, without any requirement for additional crosslinking compound. Hence, NBD can be compared with the DCPD, as the latter show similar structural features but with an additional attached cyclopentadienyl group (Figure 25).

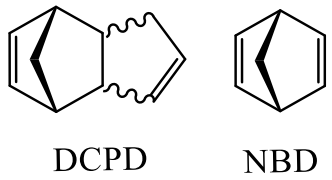

Figure 25. Molecular structure of DCPD (left) and NBD (right).

Although, DCPD polymer has been already studied both as bulk material and polyHIPE, NBD polymer has only a few publications investigating its bulk properties, while no scientific work deals with NBD polyHIPEs. The latter maybe attributed to its high price. In the present study, we tried to provide a first approach on preparing stable HIPEs that can be polymerized to solid monoliths, as well as to investigate the basic properties and finally contrast them with the respective DCPD.

The HIPEs were prepared with 20 wt% NBD and 80 wt% water by using 7 wt% of non-ionic surfactant according to the monomer. The monomer NBD, which corresponded to the external phase, was placed in a flask with the appropriate amount of surfactant. Subsequently, the water, which corresponded to the internal phase, was added dropwise under agitation into the flask. The mixture was stirred for 1h after the water addition. As soon as the emulsion was ready a solution of the catalyst M2 in toluene was added and the HIPE was cured at 40 °C for 2h. Considering that there was no information about the emulsions stability, we had to detailed investigate the ability to produce stable HIPEs. For that purpose, three non-ionic surfactants were used, named Pluronic L-121, Pluronic P-123 and Sorbitan monooleate (for study's purposes will be refer to as L-121, P-123 and Span80, respectively). The emulsions had to be stable and avoid possible coalescence that lead to phase separation for at least 2h or in other words, during their polymerization process.

Additional to NBD emulsions, the stable DCPD emulsion was prepared and underwent to the same examination procedure in order to be a reference point and to provide a valid evaluation for the NBD emulsions.

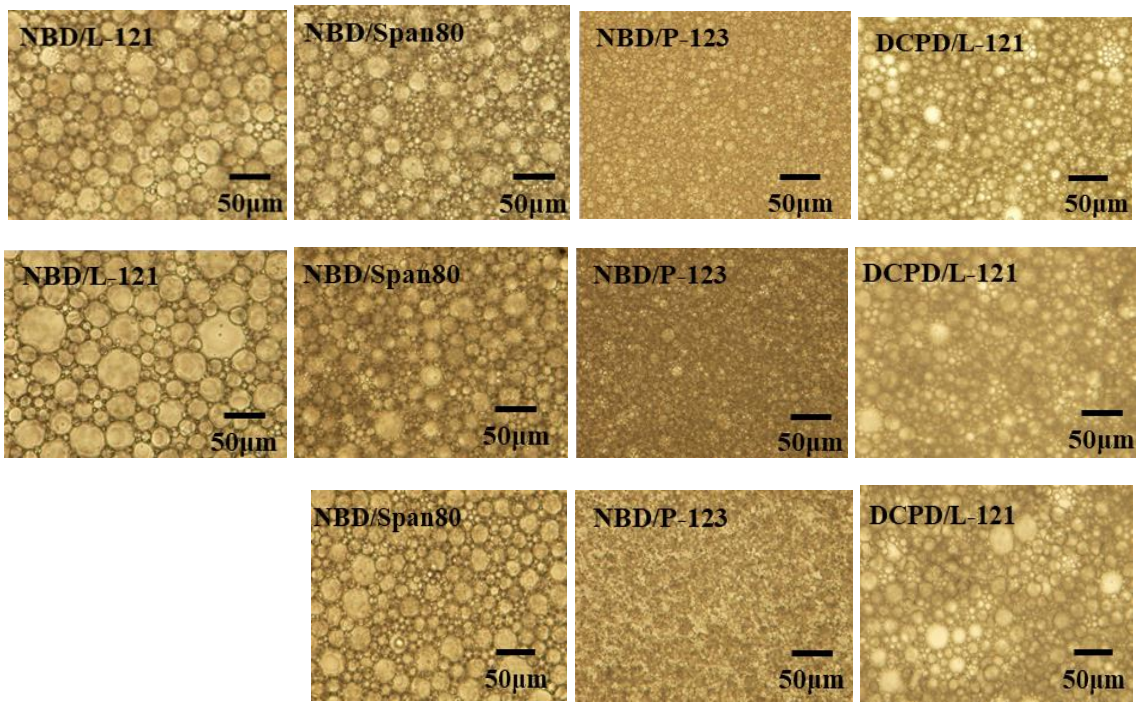

Figure 26. Optical Microscopy images of NBD/L-121, NBD/Span80, NBD/P-123 and DCPD/L-121 at room temperature at 0min (first row), at room temperature at 120 min (second row) and at 40 °C at 120 min (third row).

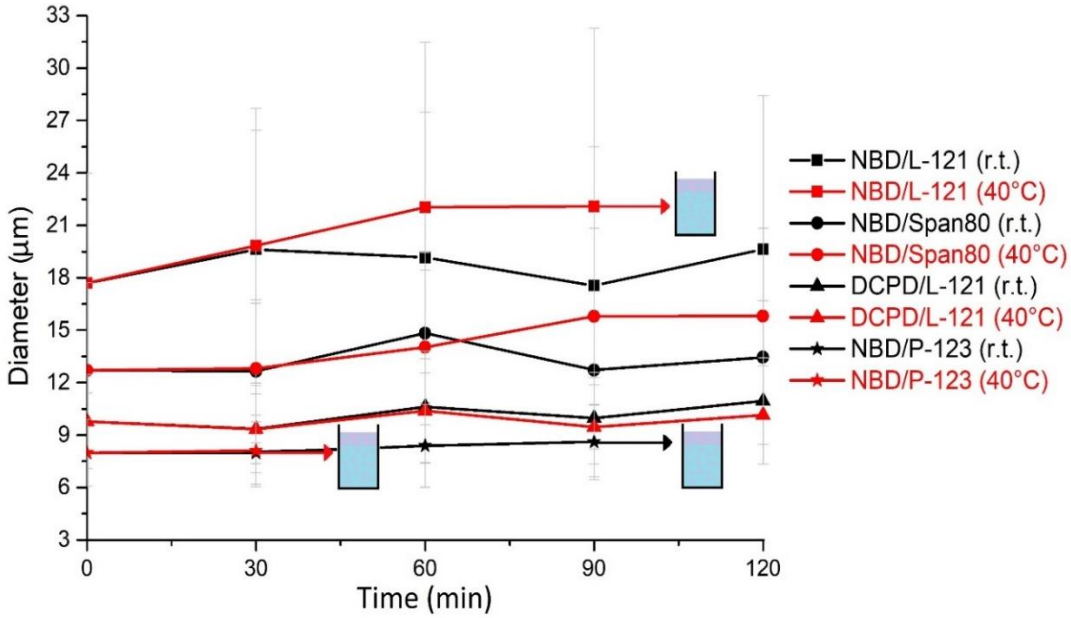

Figure 27. Droplet average size variation of NBD/L-121, NBD/Span80, NBD/P-123 and DCPD/L-121 at room temperature (r.t.) and 40 °C at 0, 30, 60, 90 and 120 min.

Figure 26 and Figure 27 illustrates the great influence of the different surfactants on the droplet size and dispersity of various HIPEs, as well as the impact of the temperature and time. Among NBD HIPEs, P-123 produces the smallest and highly monodispersed droplets. On the other hand, L-121 that belongs in the Pluronic group as P-123 but exhibits a lower molecular weight, forms droplets almost double in size compared to P-123 with a huge size distribution. Finally, Span80 provides an intermediate picture that is closer to the DCPD/L-121. The size difference and distribution between DCPD and NBD that prepared with L-121 reveal that apart from the surfactant, the type of monomer is also of great importance for the emulsion appearance. DCPD induces the formation of small droplets with decreased dispersity, while the sizes are not affected by the time and temperature. The stability studies on the three NBD HIPEs show that almost all samples at room temperature are not affected by the procedure duration, but an elevated temperature can sometimes cause negative results. Span80 produces the most stable one, as the droplets size does not change considerably within the process duration and temperature, and hence presents quite similar behavior to DCPD. Nevertheless, a tiny increase on size observed at 90 min at 40 °C, which does not lead to phase separation. On the contrary, L-121 forms less stable emulsions as the feature enlargement starts before the half way of the process, while before the process completion, phase separation could be discerned without the optical microscope.

The emulsions formed by P-123 displayed a completely different behavior under the same process. While the initial observations provide nice small and highly monodispersed droplets, after some time there was an atypical picture referred to phase separation, which was not distinguished with the naked eye and probably it was proceeded with a mechanism other than the so-called Ostwald effect and gradual size increase of droplets. It must be mentioned that the effect was presented at both temperatures, but it was obviously faster and more intense at elevated temperature.

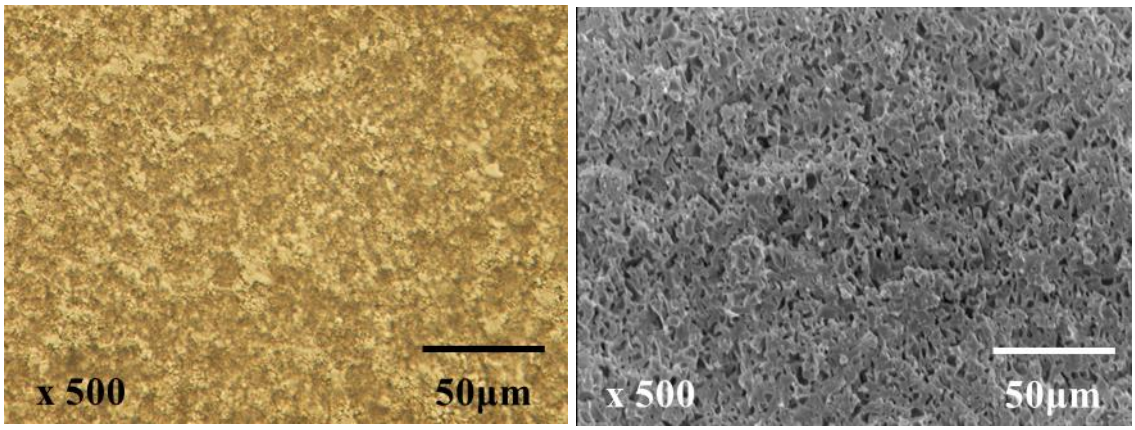

Figure 28. Optical microscopy (left) and SEM picture (right) of NBD/P-123 polyHIPE.

The SEM picture of NBD/P-123 polymer illustrates a porous material which is not a polyHIPE as it does not contain the typical voids and windows (Figure 28). This image proves the optical microscopy observations for the phase separation occurred on the emulsion at elevated temperature. The catalyst M2 used for the polymerization is activated at high temperatures quite fast, but it seems that it is not so fast to cause the polymerization within the period of time that the emulsion is stable. A production of the polyHIPE can be based on an active catalyst at room temperature or a fast catalyst that can accomplish the polymerization at 40 °C in less than 1h. Even though the P-123 is possibly able to produce polyHIPEs with small and nicely distributed voids with promising properties, the detailed study of such polymerization system was out of the scope of our work and thus, we decided to continue by investigating only the polyHIPEs resulted by L-121 and Span80.

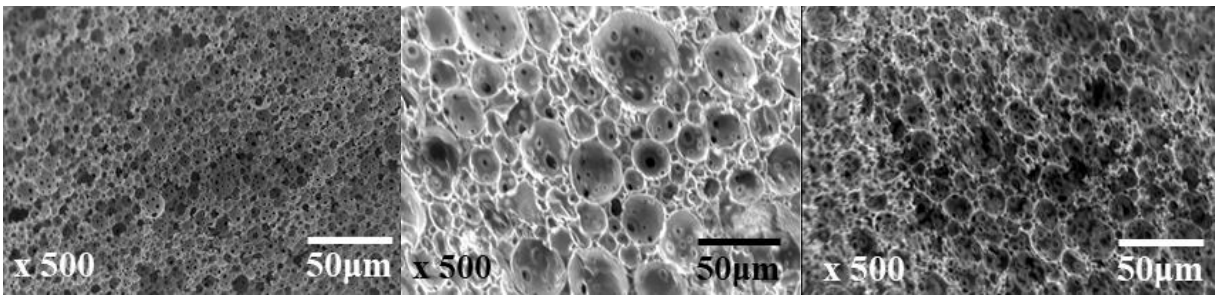

Figure 29. SEM pictures of DCPD/L-121 (left), NBD/L-121(middle) and NBD/Span80 (right) polyHIPEs.

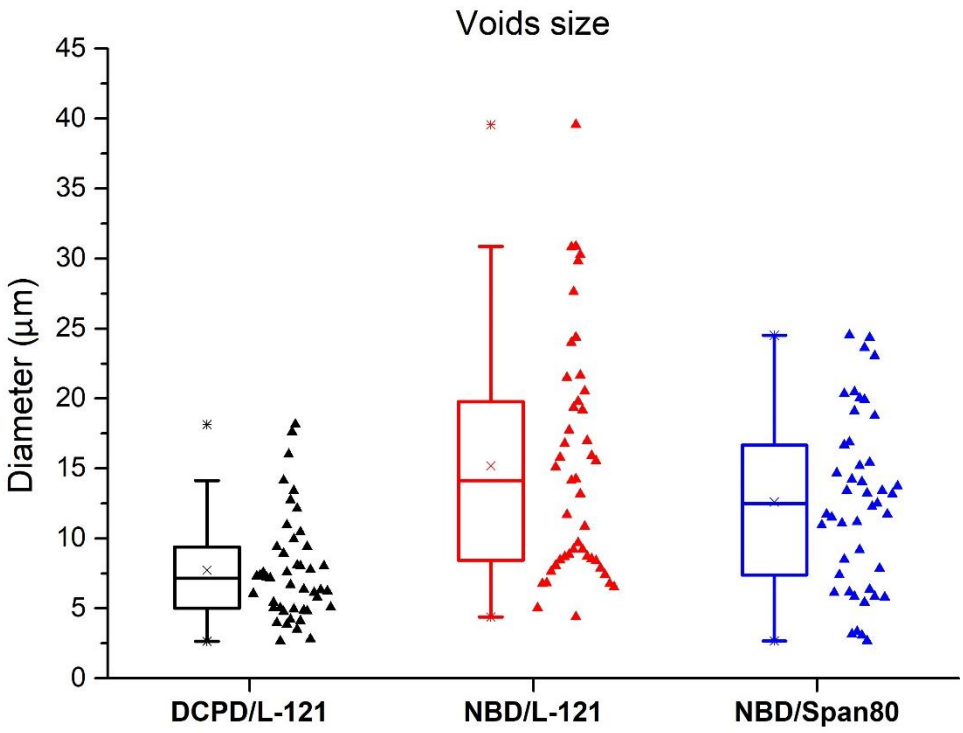

Figure 30. Box-whisker and beeswarm plots represent the data distribution referring to voids size of NBD and DCPD polyHIPE samples.

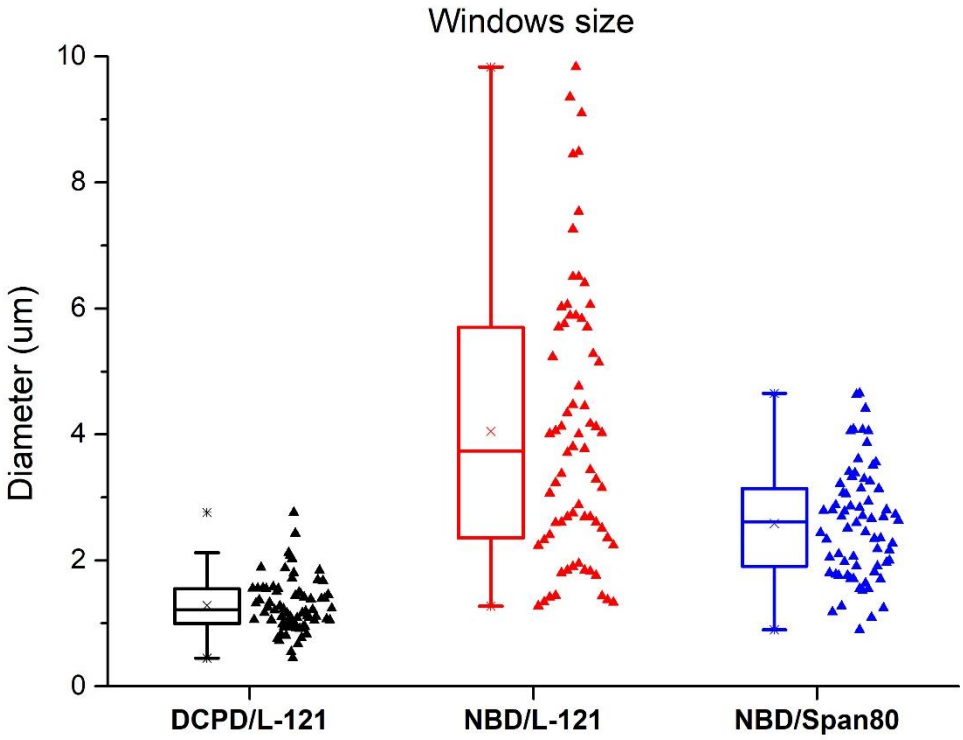

Figure 31. Box-whisker and beeswarm plots represent the data distribution referring to windows size of NBD and DCPD polyHIPE samples.

SEM pictures of NBD prepared with L-121 and Span80 (Figure 29) display the typical polyHIPE morphology of voids and numerous interconnected windows, analogous to the DCPD. The evaluation was done on the oxidized sample because they demonstrate high brittleness and there are no considerable differences on macrostructure.[7] Similar to the DCPD/CLC work, box-whisker plots combined with the beeswarm plots illustrates the size distribution of voids and windows as well as their mean size for the different polyHIPEs. The NBD polyHIPEs contain larger voids compared to respective DCPD and show a broader data distribution (Figure 30). These results are in accordance to emulsion stability studies of their HIPEs. As it is already stated before, DCPD droplets have not only the smallest size but also their size does not vary during the process. In contrast, both NBD droplets exhibit larger size and coalescence after a certain time. Nevertheless, the increased voids size can be considered as an important factor for the mechanical behavior of our polyHIPEs.

During the emulsion stability studies, it was not possible to have any information about the windows, because they are formed during the polymerization on the thinnest sides of the polymer's walls.[3,5] As a result, only SEM picture can provide us that information. By evaluating the pictures (Figure 31), we conclude that the DCPD/L-121 has the smallest windows with the narrowest distribution, while the NBD/L-121 reveal the exact opposite picture. The size differences among the polyHIPEs windows can have a great impact on mechanical properties similar to voids. To conclude, the SEM results prove the emulsion stability studies and show that not only the monomer structure but also the kind of the surfactant have a significant impact on the foam's morphology.

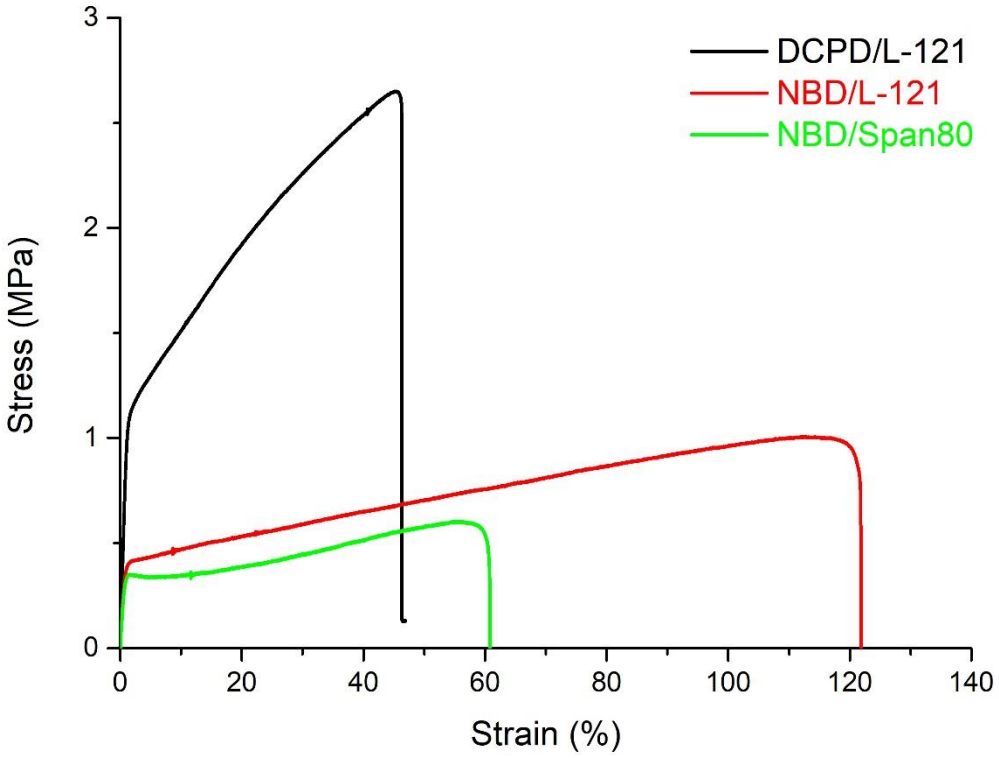

Figure 32. Curves resulted by tensile tests on unoxidized DCPD and NBD polyHIPE samples.

There are three factors that contribute the most on the mechanical behavior of the polyHIPEs, the monomer, the surfactant and the size of voids and windows. As we have already seen before, the size of the features strongly depends on the other two factors. Thus, by combining different monomers and surfactant we can govern the mechanical properties to some extent. The stress-strain curves resulted by tensile tests on DCPD and NBD polyHIPEs (Figure 32) display the huge difference between the two monomers prepared with the same surfactant. DCPD polyHIPEs can withdraw large amount of strength compared to NBD. On the other hand, NBD can achieve max elongation up to 120 %. The curves also represent the influence of the surfactants on the same polymer. In that case the maximum applied force ranges on the same level, whereas the maximum elongation for the polymer resulted by Span80 is almost the half compared to the polymer resulted by L-121.

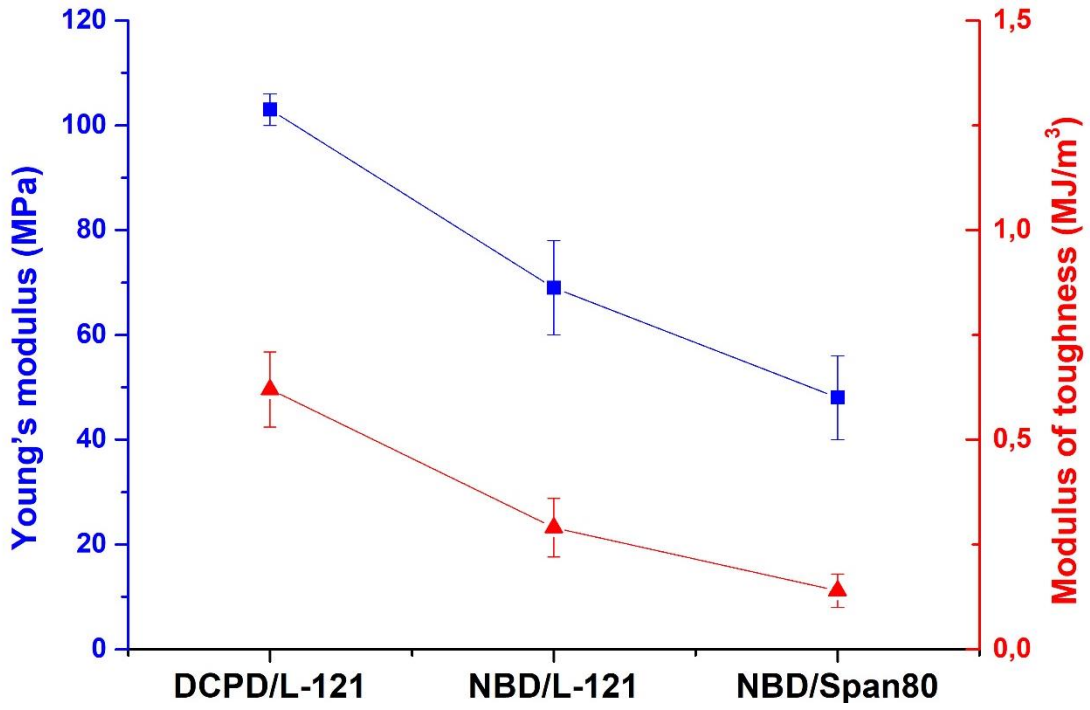

Figure 33. Young's modulus and modulus of toughness relation among DCPD and NBD polyHIPEs.

Similar behavior is followed by the Young's modulus and modulus of toughness (Figure 33). DCPD polyHIPEs continues to exhibit by far the largest moduli and can be characterized as highly stiff and tough materials. NBD polyHIPEs, on the other hand, demonstrate lower moduli than DCPD, but they are still stiffer than the most studied polyHIPE material, styrene-co-divinylbenzene (Young's modulus below 30 MPa).[18] The overall mechanical behavior described above for the three polyHIPEs is the direct outcome of the different monomers that have discrete ring strain and hence ability to form polymers and crosslinking bonds, as well as of the surfactant kind. More specifically, the two different surfactants have an essential role on the mechanical properties. Studies showed that L-121 surfactant can be completely removed from the final polyHIPE, while the Span80 tends to be covalently incorporated into the polymer chain. The double bond on the molecule can participate in cross metathesis reactions with the double bonds of the monomers and polymer chain.[19] Thus, Span80 can change the arrangement of the polymer network.

Finally, different microporous structure also contributes to the overall mechanical behavior. SEM analysis showed that NBD polyHIPEs exhibit notable differences on their morphology. More specifically, the bigger voids of NBD/L-121 renders them stiffer, because the same amount of

monomer as in NBD/Span80 has to be accommodated in a same space area. This indicates that some amount of the monomer is accumulated in-between the voids, leading to more rigid materials. The Young's modulus in Figure 33 perfectly depicts the above. The windows also follow the same size trend as the voids. Although, the bigger windows lead to more brittle materials, the NBD/L-121 with the bigger windows has more pronounced elongation than NBD/Span80. It seems that in terms of material's flexibility, factors other than the window's size contributes more drastically.

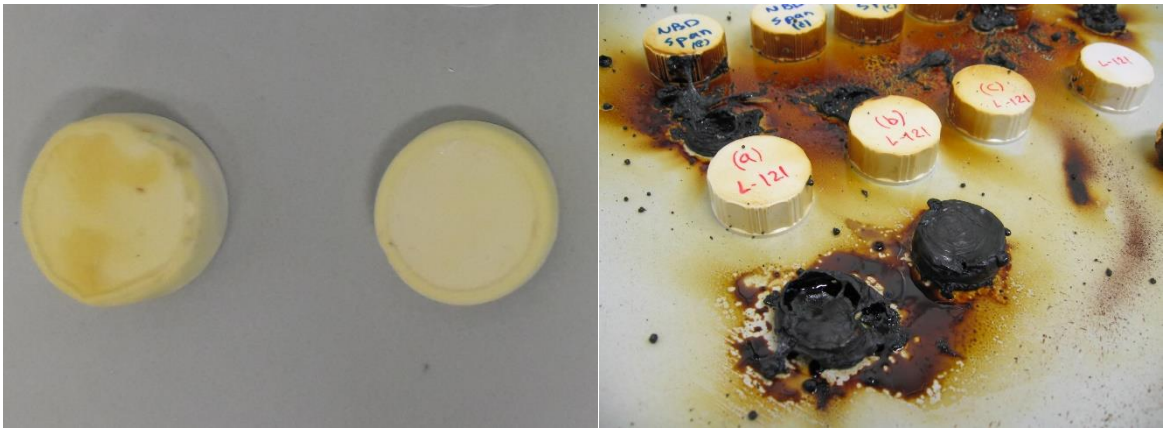

Figure 34. NBD polyHIPEs after 1h (left) and 24h (right) exposure to ambient conditions.

An interesting property of NBD polyHIPEs is the fast oxidation under ambient conditions. DCPD and NBD polyHIPEs have a high content of double allylic positions which easily react with the atmospheric O_2. DCPD polyHIPEs, though, have quite low reactivity, as they need either one month at ambient conditions or 24h at 40 °C, in order to get fully oxidized. The oxidation can be recognized either by their yellow color or by an IR measurement. IR spectra of oxidized DCPD foam exhibit two typical peaks, a broad one at 3400 cm^{-1} attributed to O-H and a sharp at 1700 cm^{-1} because of the C = O formation during oxidation.[6] On the contrary, NBD foams turned to yellow quite fast, after their preparation and turned out to be liable to ignite spontaneously, during drying under ambient conditions. (Figure 34).

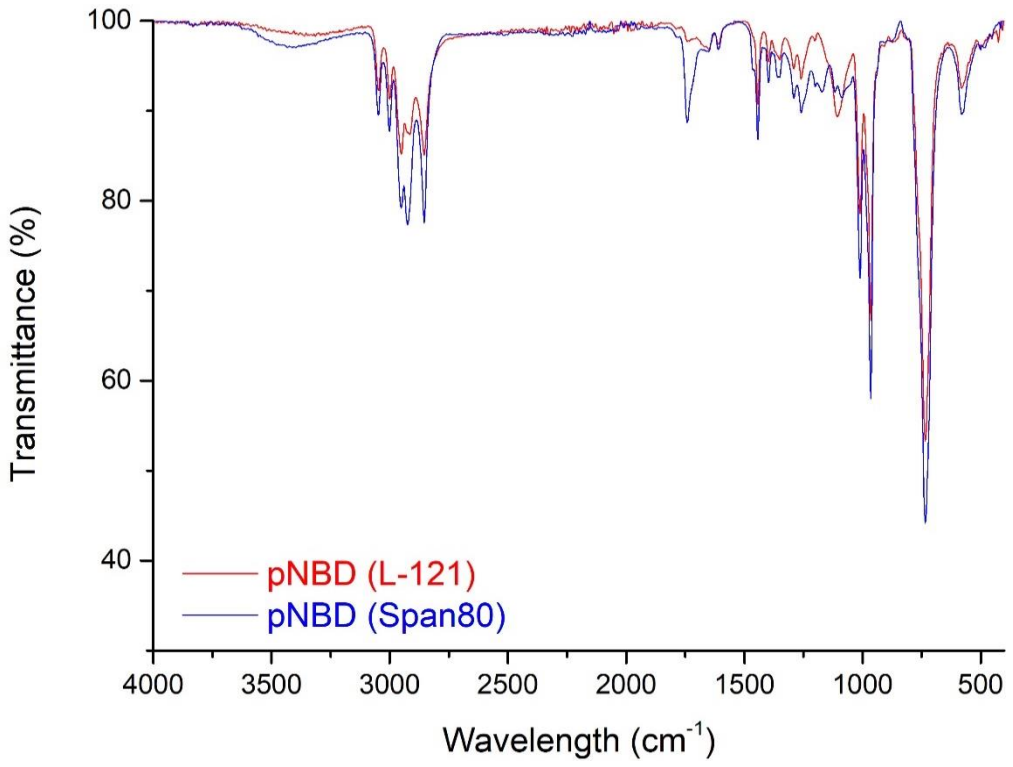

Figure 35. IR spectra of unoxidized NBD/L-121and NBD/Span80 polyHIPEs.

IR spectra analysis of the two unoxidized NBD polyHIPEs (Figure 35) show similarities but also differences. More specifically, there are two sharp peaks positioned at 735 and 965 cm^{-1} for both NBDs. By reading the IR spectra of already studied polymers such as polybutadiene which contain many double allylic bonds and are quite similar to our NBD polymers, it can be concluded that these two peaks correspond to cis C = C and trans C = C absorptions, respectively.[20] The high intensity of these two bands, matches to the fact that the samples are unoxidized and contain a large amount of double bonds. On the other hand, NBD/Span80 foam displays two peaks at 3400 cm^{-1} and 1700 cm^{-1} that are not found in case of NBD/L-121. The existence of these peaks is possibly attributed to the covalently bonded surfactant. If we compare the specific spectra with the IR spectra of surfactant Span80 (Figure A1, Figure A4), the peaks are on the same position. This outcome proves the presence of the surfactant on foams and hence explains further the tensile test results referring to NBD prepared with Span80. Although, theoretically the surfactant L-121 should be completely removable, on the NBD/L-121 graph it can be clearly pointed on hand of the absorption peaking at 1100 cm^{-1} (attributed to C-O-C vibration, Figure A1, Figure A2), which

reveals that during the foams production, L-121 was not completely removed. IR spectra of unoxidized NBD/L-121and NBD/Span80 polyHIPEs.

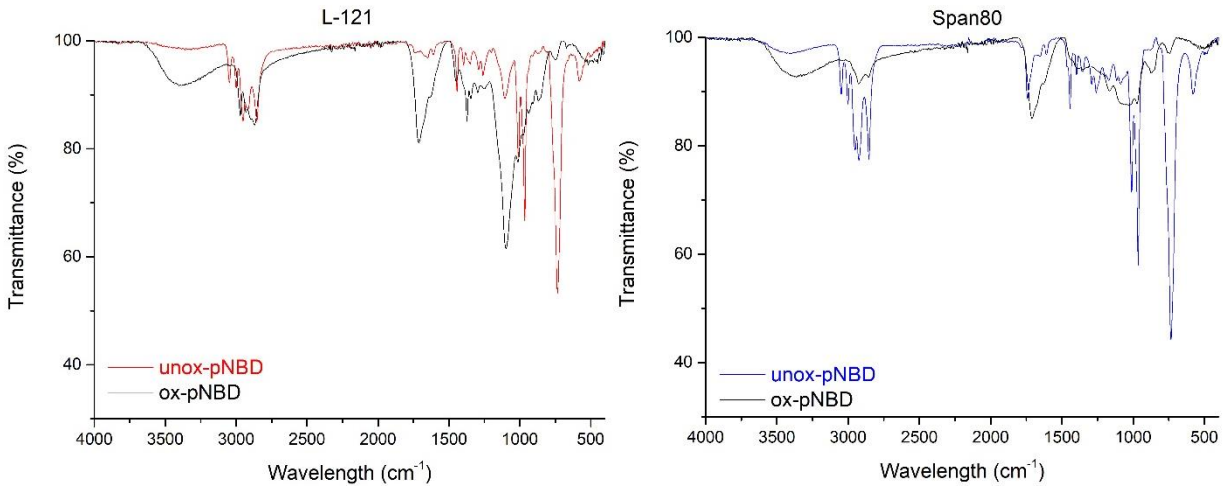

Figure 36. IR spectra of unoxidized and oxidized NBD/L-121(left) and NBD/Span80(right) polyHIPEs.

In order to prove that the yellow color on NBD polyHIPEs is ascribed to oxidation, we compared the IR spectra of unoxidized and oxidized NBD foams (Figure 36). Both spectra of oxidized species have the typical peaks at 3400 cm^{-1} and 1705 cm^{-1} similar to oxidized DCPD, which ascribed to – OH and C = O absorptions, respectively.[6] As mentioned before, the unoxidized NBD/Span80 demonstrates these two peaks with lower intensity due to the surfactant, whereas NBD/L-121 sample has not any peak at those areas. Moreover, the sharp bands at 735 and 965 cm^{-1}, appeared on IR spectra of unoxidized samples, seem to disappear almost comletely. This is may be attributed to the double bond consumption due to the oxidation.

The scientific proof for the oxidation from IR spectra and the observation that the NBD samples react fast with the atmospheric O_2 can incorporate them into the category of oxygen scavengers. The O_2, even though, is very important for the living organisms, sometimes is very destructive for chemical and biological compounds but more specifically, it can be a serious enemy for food products. The oxygen scavengers or oxygen absorbers are able to protect the quality of the food product from several biological and chemical reactions take place due to the O_2 presence. The oxygen scavengers have a great demand on modern markets. There are two large groups of oxygen absorbers, the metallic and nonmetallic. The metallic group contains the most popular iron-based scavenger. These scavengers are usually used as powders in sachets, which are permeable only to O_2. The mechanism encloses the formation of hydrated metallic reducing agents, after the reaction

of the iron-based compounds with the water from the food product. The highly reactive reducing agents, then, react with the O_2 in the food package and produces a stable oxide. Although, the iron-based scavengers can provide conditions with less than 0.01% O_2, they represent two disadvantages. The first refers to the possibility of causing a serious contamination on the food product, while the second signifies the limited use on beer, wine and the rest beverages due to the high water activity, which hinders the activation process and as a result the scavenger losses its ability to remove the oxygen. These disadvantages are overcome with the nonmetallic oxygen scavengers. This group contains the rest types of scavengers including organic and enzymic compounds.[21]

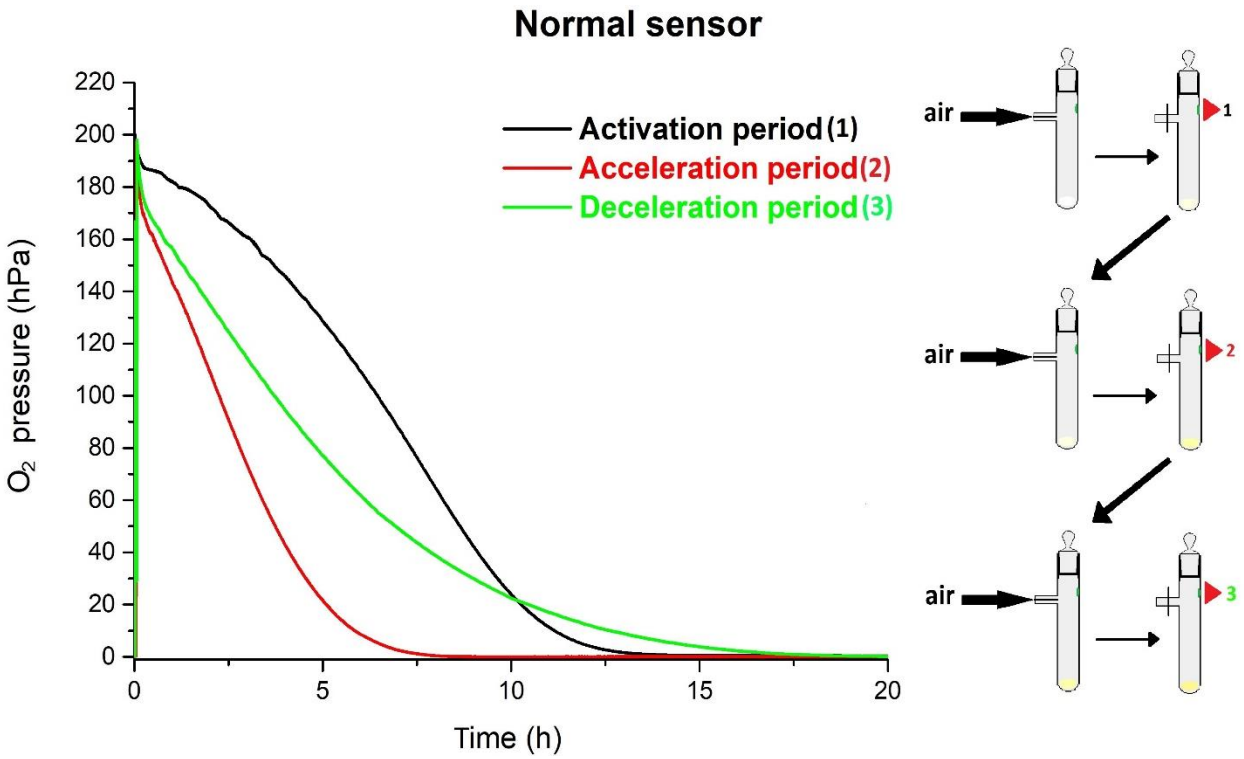

Figure 37. Oxygen measurement (normal sensor) on big NBD polyHIPE sample with atmospheric O_2 under ambient conditions, exhibiting the typical oxidation behavior of olefinic materials(left) and the scheme for the measurement procedure(right).

All the above information for the already established oxygen scavengers, as well as our observations and IR results triggered us to record the behavior and rapidity till complete oxidation, as well as the amount of O_2 consumed. The experiment was carried out with atmospheric O_2 (20.95%) under ambient conditions by using an optical oxygen sensor, which collects data for the O_2 concentration in a container by monitoring the luminescence lifetime.[22] The measurement was

firstly accomplished on relatively big NBD samples with a normal sensor (reliable limits 1000hPa-1hPa). The flask, where the monolith was placed, had to be filled thrice with fresh air in order to reach complete oxidation because there was an excess amount of material compared to the amount of O_2 within one single flask. The three curves on Figure 37 represent a typical oxidation behavior of olefinic materials such as polybutadiene. Nevertheless, it must be mentioned that the oxidation of olefinic materials usually occurs at elevated temperatures compared to NBD polyHIPEs. The black curve is the slow activation period, where the necessary amount of radical is formed by autoxidation reaction. The red curve represents the acceleration period. At that point, the appropriate amount of radicals has been already produced and the reaction occurs fast, leading to hydroperoxide formation, even if the O_2 concentration is considerably low. Activation and acceleration period correspond to an autocatalytic reaction. Last but not least, the green curve denotes the deceleration period, where the reaction is slowing down. The initial part of the last curve show that the reaction is similarly fast to the acceleration period but the end of it display a reaction slower than the activation period. There are three possible explanations for this behavior, the reduction of the available positions on the foam, the decay of the hydroperoxide amount due to decomposition and the oxidation rate decrease due to limited O_2 diffusion. Nevertheless, the deceleration period can be caused not only by one factor but by combining two or more.[23]

A special issue with the normal sensor is the detection limit at low O_2 concentrations. More particularly, the normal sensor can provide a reliable signal within the O_2 pressure 1000 hPa and 1hPa. This indicates that the values below 1 hPa measured by the normal sensor do not correspond to valid values. Accordingly, there are no information if the conditions in the flask are anoxic or to what extent the O_2 consumption can be proceeded when the concentration is significantly low. For that reason, a second more sensitive sensor (perfluoroalkylated Pt, Teflon AF 1600)[26] was used simultaneously with the normal sensor. This additional trace sensor has a reliable pressure range between 50 hPa and 0.003 hPa. The lower limit of 0.003 hPa corresponds to approximately 0.0003% (3 ppmv) O_2. Our samples have the ability to reach the lower limit of 0.0003% O_2 within a container. This outcome makes the NBD polyHIPEs capable to reduce approximately 2 orders of magnitude more the amount of O_2 compared to the already established O_2 scavengers.

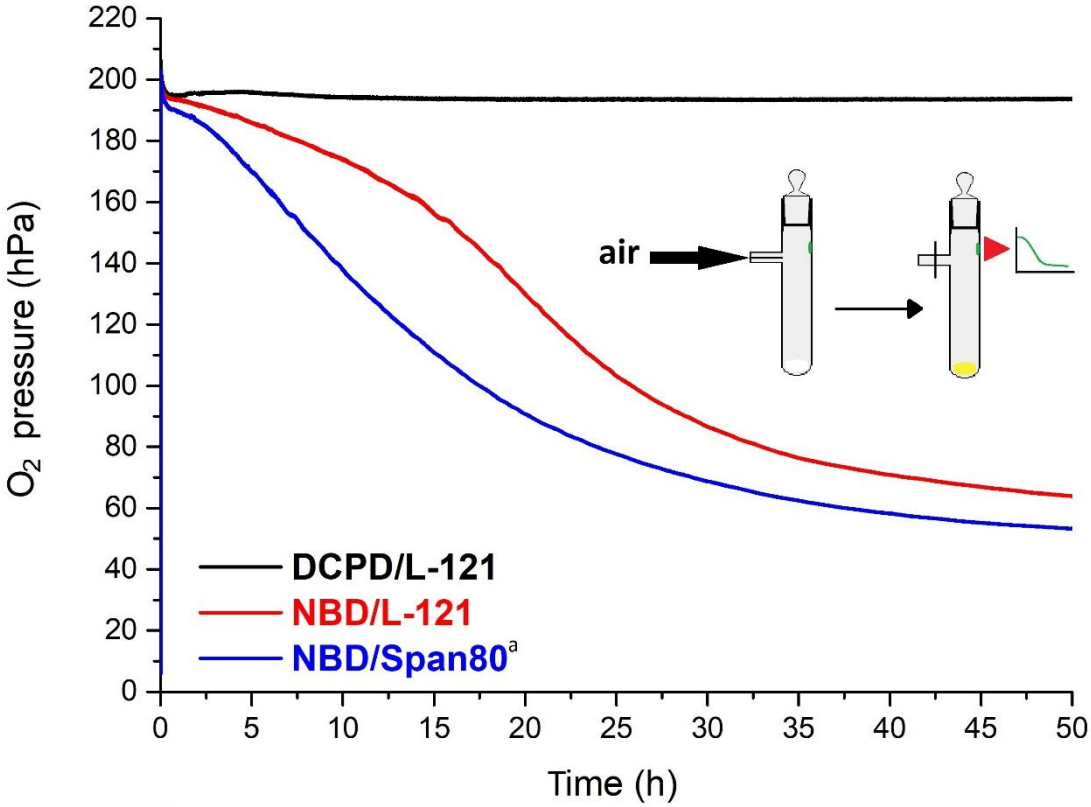

Figure 38. Oxygen measurement (normal sensor) on small NBD and DCPD polyHIPE samples with atmospheric O_2 under ambient condition and the scheme for the measurement procedure.

The repetition of the oxygen measurement on small (approximately 1/6 of the big samples weight) NBD polyHIPE samples resulted the same behavior but in one single curve. Compared to big samples, in that case the amount of O_2 was in excess and as a result, the experimental flask was filled only once with fresh air for each measurement. As it can be illustrated by Figure 38, both NBD samples demonstrate three different part on one displayed curve, an activation period in the beginning, an acceleration period in the middle and a deceleration period in the end. The difference between the two NBD sample and specifically the short activation period appeared on NBD/Span80 is possibly ascribed to a minor oxidation before the measurement. The NBD prepared with Span80 always exhibited a degree of oxidation (light yellow color) during their storage under nitrogen in contrast to NBD/L-121, and hence it was difficult to handle them properly. Moreover, the different behavior is attributed to the different weights (Table 2). The small samples were derived by cutting the big samples and thus it was hard to recut the exact same

weight. Nevertheless, the heavier sample has additional available oxidation positions and therefore consumes more O_2.

For the full oxidation of DCPD polyHIPEs, it is known that under ambient conditions at least one month is needed. Unfortunately, this information is provided only by observations and there was not any valid measurement to allow us the comparison with NBD samples. Thus, we performed an oxygen scavenging experiment under the same conditions with a NBD polyHIPE and the result is also illustrated in Figure 38. The curve shows that the O_2 indication for DCPD remains unchanged for at least 50h, while on the same time the NBD samples have already been saturated. This outcome indicates how fast the NBD samples can consume an amount of O_2 from a defined container.

Finally, it was important to determine the amount of consumed O_2. The reaction of NBD samples with the O_2 changes, except for the appearance (yellow), also their weight. Thus, by weighting the samples before and after the measurements, we were able to note the difference and calculate the amount of O_2. Table 2 presents the oxygen measurement results and calculations for the big and small samples, as well as the volume of flask and the amount of available O_2 in it, used for each measurement. The measurements reveal that the wt% increase ranges from 23 to 24 % and corresponds to O_2. If the additional O_2 weight is translated to moles, it is obvious that nearly every repeating unit (RU) on the polymer reacts with one O_2 molecule and consequently, it is approximately a 1 : 1 reaction. Nevertheless, it must be considered that sometimes it is difficult to achieve full oxidation because of the polyHIPE morphology, that hinders the O_2 diffusion into tiny voids, especially when its amount in the flask is significantly low. Therefore, it is able to cause rapidly almost anoxic conditions within containers of known volume, only by preparing NBD polyHIPEs of a certain weight.

We already mentioned before that in case of the big sample, the flask was filled thrice because all the amount of O_2 was removed. Three flasks, then, corresponds to approximately 170 mL O_2. On the other hand, the weight measurements give a mass increase of 130 mL. This difference may be attributed to the fact that in the beginning the oxidation induces the formation of hydroperoxides, but, because the hydroperoxides are not stable some of them are decomposed leading to the formation of other oxygen compounds such as carbonyls and hydroxyl groups.[7,10] The

decomposition is possibly connected to the release of water or other volatile compounds, which could explain the difference between the two volumes.

Table 2.The volume of flask and weight of samples used for each measurement, weight, wt% increase and oxygen consumption after measurement, as well as reaction ratio.

	NBD/L-121 (big)	***NBD/L-121 (small)***	***NBD/Span80 (small)***
Experimental flask, mL (20.95% O_2, mL)	270 (56.57)[a]	270 (56.57)	270 (56.57)
Start, g (mmol)	0.6258 (6.8)	0.1135 (1.2)	0.2206 (2.4)
End (g)	0.8115	0.1482	0.2945
wt% increase	23	23	25
Consumed O_2, g (mmol)	0.1857 (5.8)	0.0347 (1.1)	0.0739 (2.3)
Consumed O_2, mL	130.0	24.3	51.7
RU : O_2	1 : 1.2	1 : 1.1	1 : 1.0

[a] The same flask was filled thrice for the measurement.

3.2.2 Conclusion 2

In the current work, we prepared for the first time HIPEs consisting of the monomer NBD, water and non-ionic surfactants. For that purpose, three emulsions were prepared by using three different surfactants, Pluronic L-121, Pluronic P-123 and Sorbitan monoolate (Span80). The examination of the emulsion stability under ambient and polymerization conditions revealed that L-121 and mostly Span80 are able to produce stable emulsions and thus, polymeric foams after curing procedure. The SEM measurements show differences in feature sizes between NBD prepared with different surfactants, a result that is attributed to the emulsion stability. Tensile tests concluded to the outcome that NBD polyHIPEs are less stiff and tough compared to the respective DCPD but they showed higher elongation. Last but not least, observations and IR measurements presented a fast oxidation of the NBD foams under ambient conditions, which induce oxygen measurement on the NBD samples. These measurements exhibited that the oxidation follows the typical behavior of olefinic compounds as well as that roughly every repeating unit reacts with one O_2 molecule.

4 Experimental section

4.1 Materials

Dicyclopentadiene (DCPD, Aldrich), Norbornadiene (NBD, Alfa Aesar), Pluronic®L-121 and Pluronic®P-123 (poly-(ethylene glycol)-block-poly(propylene glycol)-block-poly-(ethylene glycol), Aldrich), Span80 (Sorbitane monooleate, Aldrich), the initiator ($H_2IMes)(PCy_3)Cl_2Ru$(3-phenyl-indenylid-1-ene) (M2, Umicore's 2nd generation initiator, H_2IMes = *N,N-bis-(mesityl) 4,5-dihydroimidazol-2-yl*, PCy_3 = *tricyclohexylphosphine*), ethanol (Aldrich), acetone (Aldrich) toluene (Aldrich) and n-pentanol (Fischer Scientific) were used as received. CLC was prepared according to the literature (Christina Wappl, Master Thesis, TU Graz 2013).

4.2 Common characterization methods

IR spectra results were taken on a ALPHA FT-IR Spectrometer from Bruker. The morphology of the polyHIPEs was examined by scanning electron microscopy (SEM) with JWS-7515 JEOL ltd. microscope. The measurements were done on the oxidized species as it was too difficult to break or cut the sample without destroying the porous structure. The DCPD monoliths were oxidized at 40 °C overnight, while the NBD monoliths were oxidized at ambient conditions overnight. The resulted oxidized species were brittle enough without considerable morphological differences.[7] Thus, the samples were broken and mounted on a carbon tab for better conductivity and a thin layer of gold was sputtered on the sample's surface before the scanning analysis. Micrographs were monitored at several magnifications from 500 to 2000 fold, at 7 mm working distance and at 20 kV acceleration voltages. The evaluation of the voids and the windows was defined by the SEM pictures after scanning. The diameter of at least 50 voids and 70 windows was measured manually in order to give the mean value and the standard deviation as well as the data distribution. Due to the improper cut of the samples, it was difficult to correctly evaluate the sizes. Consequently, voids and windows' diameters had to be multiplied with the correction factor $2/3^{1/2}$. Thermogravimetric analysis (TGA) of the DCPD/CLC polyHIPEs and bulk copolymers was performed with a Netzsch Simultaneous Thermal Analyzer STA 449C (crucibles: aluminium from Netzsch) under nitrogen flow. The heating rate until a final temperature of 550 °C was 10 °C/min. For mechanical testing the HIPEs were prepared as descripted in 4.3.1 and 4.4.1 and casted in Teflon moulds (shouldered tensile test specimens, of 5 mm width at breaking point, thickness of 3 mm, 43 mm gage length,

62 mm distance between shoulders and 100 mm overall length, Figure 39). Tensile tests of polyHIPEs were performed at room temperature on an electromechanical universal testing machine (AGS-X by Shimadzu) equipped with a 50 kN load cell. DCPD/CLC samples were tested at a test rate of 10 mm/min, while NBD samples were tested at a rate of 5 mm/min. The mean Young's moduli were calculated from data obtained from the initial linear slope of the stress-strain plot with at least four samples of the same composition.

Figure 39. Teflon moulds used for tensile bars preparation

4.3 Dicyclopentadiene (DCPD)/Crosslinking Comonomer (CLC): Preparation and specific characterization

4.3.1 High Internal Phase Emulsion co-polymerization

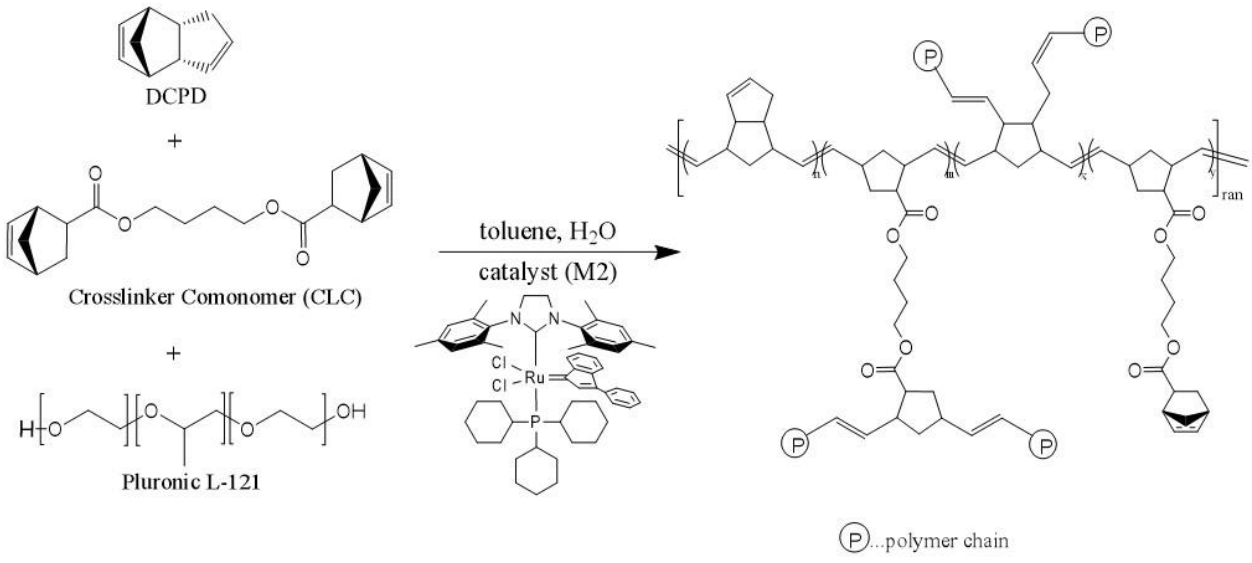

Figure 40. Scheme of DCPD/CLC polymerization after the emulsion preparation with surfactant L-121.

The water amount can be calculated by the following equation:

$$porosity\ \% = \frac{m_{H_2O}}{m_{H_2O} + m_{monomers} + m_{toluene}}$$

A series of foams of 80% nominal porosity was prepared by **DCPD** and a varying content of a second crosslinking comonomer (**CLC**) (10-40 wt% in respect to DCPD). the DCPD homopolymers was also prepared. In a 250 mL three necked round bottom flask, a total amount of 10 g of monomers and 0.7 g of Pluronic L-121 surfactant (7 wt% in respect to the total amount of monomers) were weighted. Moreover, 100 mL toluene were added in order to maintain the DCPD in liquid state. Afterwards, the mixture was stirred with a mechanical stirrer at 400rpm while 40 mL distilled water were added dropwise. After water addition, the mixture was turned into milky, viscous emulsion and the stirring was carried on for one hour. Catalyst [1,3-Bis (2,4,6-trimethylpheny-l-2-imidazolidinylidene]dichloro (3-phenyl-1H-inden-1-ylidne)(trichloro-hexyl-phosphine)ruthenium(II) (M2) with molar ration of 1:15000 (regarding both monomers on each sample preparation) was dissolved in 200 μL toluene and was added to the emulsion under agitation. The pinky mixture was poured into moulds and cured at 80 °C for 3h. Finally, the white samples were placed in acetone for 15 min in order to remove the surfactant and dried under ambient conditions.

Table 3. DCPD, CLC and catalyst amount in grams and moles for the synthesis of homo- and co-polymer polyHIPEs.

	DCPD, g (mmol)	***CLC, g (mmol)***	***Catalyst, mg (mmol)***
P0	10 (75.6)	-	4.8 (0.0050)
P10	9 (68.1)	1 (3.0)	4.5 (0.0047)
P20	8 (60.5)	2 (6.1)	4.2 (0.0044)
P30	7 (52.9)	3 (9.1)	3.9 (0.0041)
P40	6 (45.4)	4 (12.1)	3.6 (0.0038)

4.3.2 Bulk copolymerization

A series of bulk copolymers by **DCPD** and a varying content of a second crosslinker comonomer (**CLC**) (10-40 wt% in respect to DCPD), as well as the homopolymers of DCPD and CLC were

prepared. In a 20 mL vials, a total amount of 1 g of monomers was weighted. Furthermore, 50 μL toluene were added into vials contained DCPD in order to prevent its solidification. Catalyst [1,3-bis(2,4,6-trimethylpheny-l-2-imidazolidinylidene]dichloro(3-phenyl-1H-inden-1-ylidne) (trichloro-hexyl-phosphine)ruthenium(II) (M2) with molar ration of 1:15000 (regarding both monomers on each sample preparation) was dissolved in 50 μL toluene and was added to the monomer mixtures. The later were polymerized at 80 °C for 2h. The resulted homo- and co-polymers were undergone IR and TGA measurements in order to be compared with the respective polyHIPEs.

Table 4. DCPD, CLC and catalyst amount in grams and moles for the synthesis of bulk homo- and co-polymers.

	DCPD, g (mmol)	***CLC, g (mmol)***	***Catalyst, mg (mmol)***
B0	1 (7.6)	-	0.48(0.0005)
B10	0.9 (6.8)	0.1 (0.3)	0.45(0.0005)
B20	0.8 (6.0)	0.2 (0.6)	0.42 (0.0004)
B30	0.7 (5.3)	0.3 (0.9)	0.39 (0.0004)
B40	0.6 (4.5)	0.4 (1.2)	0.36 (0.0004)
CLC (polymer)	-	1 (3.0)	0.19 (0.0002)

4.3.3 Optimization of polymerization conditions

The conditions for the DCPD polyHIPEs production were already known from literature but due to the fact that a second monomer was added for synthesizing the copolymers, the conditions was necessary to be readapted. The following procedure was carried out five times for the five different copolymer compositions. After the HIPE preparation (4.3.1), eight disk moulds (thickness of 2 mm and diameter of 30 mm, Figure 41) were filled with the emulsion and cured at 80 °C for 2, 3, 4, 5, 6, 7 and 24h, respectively. The disks were weighted before and after the emulsion addition and after every polymerization. Afterwards, the samples were placed into acetone for 15 min and let dry under ambient conditions. The dimensions and weight of dry samples were recorded as well.

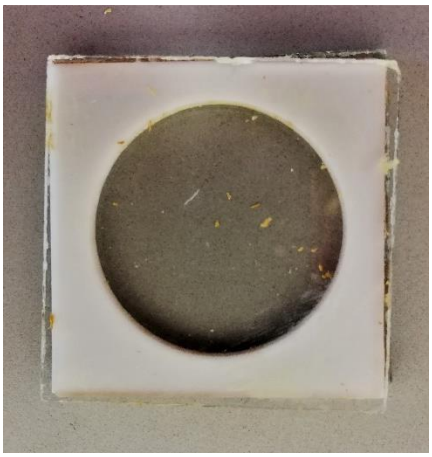

Figure 41. Disk mould used for swelling/deswelling procedure

Furthermore, the appearances of the samples that resulted by different curing durations were taken into consideration. Long polymerization time was led to considerably high water elimination and consequently to significant oxidation (yellow/brown color) (Figure 42). This situation was seemed to be slightly minimized by the rising amount of the CLC (Figure 43). The polymerization duration for the five differently composed copolymers should have been the same in order to end up to comparable results. Thus, by considering the differences in masses and colors as well as by the fact that the crosslinking degree would have reached in a satisfying level for all the samples, the curing time was set at 3h.

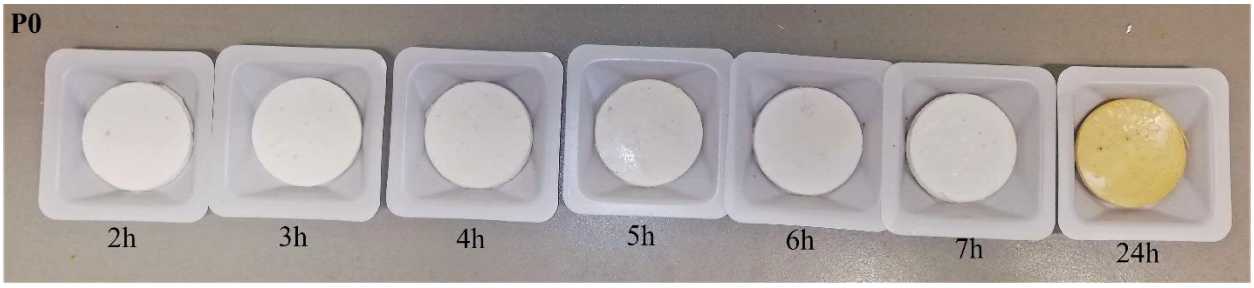

Figure 42. DCPD homopolymerization for 2, 3, 4, 5, 6, 7 and 24h (left to right).

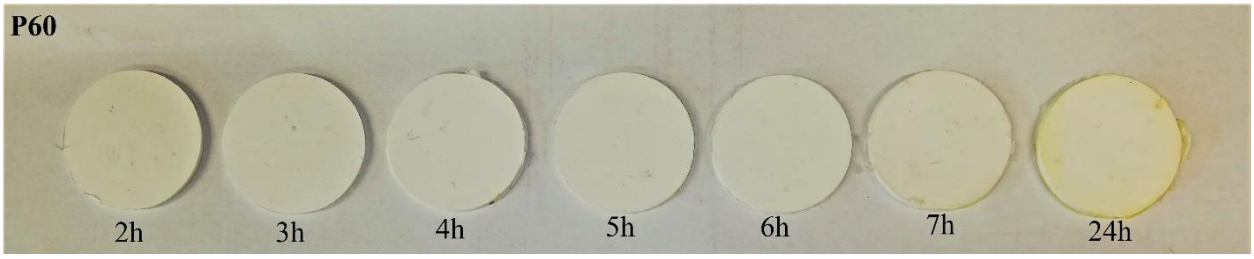

Figure 43. 60 wt% DCPD/40 wt% CLC copolymerization for 2, 3, 4, 5, 6, 7 and 24h (left to right).

4.3.4 Swelling/deswelling procedure

The HIPEs for every copolymer composition were prepared according to 4.3.1. The emulsion was poured into five disk moulds (thickness of 2 mm and diameter of 30 mm, Figure 41) and cured for 3h at 80 °C. Accordingly, the samples were placed into acetone for 15 min and dried at ambient conditions. The weight and dimensions of dry samples were recorded. Five solvents exhibiting different polarities at room temperature, water (dielectric constant ε = 80), ethanol (ε = 25), n-pentanol (ε = 15), acetone (ε = 21) and toluene (ε = 2.4),[24] were used for swelling/deswelling measurements. The copolymers were immersed into the five solvents for 24 h and following, the dimensions and weight of wet samples were received. By calculating the volume for the dry and wet samples it was possible to determine the volume % increase and therefore the swelling degree. Also, the difference between the dry and wet mass corresponded to the solvent wt % uptake. Following, the wet samples were submerged into acetone for 10 min and let dry under ambient conditions. The dimensions of the dry samples were measured in order to result the volume % decrease or in other words the deswelling degree. The above procedure was repeated for the five different compositions.

4.3.5 Porosity and density determination

Swelling/deswelling procedure showed that there was little or no increase in volume in case of samples immersed in ethanol and water. Regarding the mass of dry (m_o) and wet (m_t) samples, as well as the volume of dry samples (V_o), it was possible to calculate the porosity and hence the density (ρ) of each HIPE copolymer, as the solvent was occupying only the voids within the monoliths without causing significant swell. The porosity was calculated by using the following formula[25]:

$$porosity\ \% = \frac{m_o - m_t}{\rho \cdot V_o}$$

The density of the copolymers (not the foams) was calculated by the following formula:

$$\rho = \frac{m_o}{V_o - \left(V_o \cdot \frac{80\ \%}{100}\right)}$$

4.3.6 Determination of the crosslinked moieties fraction and CLC crosslinking degree

TGA curves were used for the crosslinked moieties fraction and CLC crosslinking degree determination. More particularly, the calculation proceeded by considering the range of second mass loss occurred at 240 °C. This mass loss is attributed to the so called Retro-Diels-Alder reaction on the free norbornene moieties of the CLC molecule which causes the elimination of the cyclopentadiene (Cp) molecule. By taking into account the respective mass loss % and molecular weight of the repeating unit (MW_{RU}), the molecular weights of Cp (MW_{Cp}) and the number of CLC exist on each repeating unit (n = 1, 2, 3 and 4), we calculated the fraction of the crosslinked norbornene moieties for each polyHIPE sample by the following equation:

$$crosslinked\ moieties\ \% = 1 - \frac{mass\ loss\ \% \cdot MW_{RU}}{MW_{Cp} \cdot n}$$

The CLC crosslinking degree was calculated in each case by the respective crosslinked moieties fraction and wt% CLC with the following formula:

$$CLC\ crosslinking\ degree = \frac{crosslinked\ moieties\ \% \cdot wt\%\ CLC}{100}$$

4.4 Norbornadiene (NBD): Preparation and specific characterization

4.4.1 High Internal Phase Emulsion polymerization

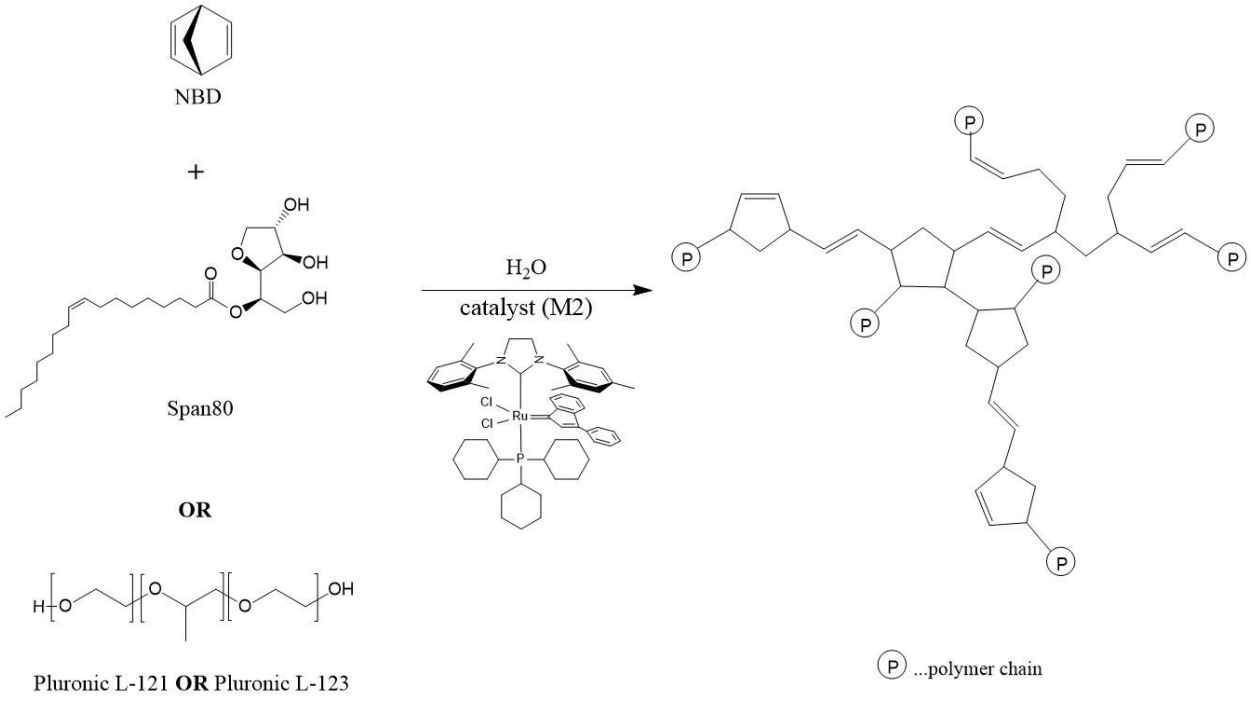

Figure 44. Scheme of NBD polymerization after the emulsion preparation with surfactant L-121 or P-123 or Span80.

The water amount can be calculated by the following equation:

$$porosity\ \% = \frac{m_{H_2O}}{m_{H_2O} + m_{NBD}}$$

Foams of 80% nominal porosity were prepared by **NBD** with three different surfactants, Pluronic L-121 and P-123 and Span80. In a 250 mL three necked round bottom flask, 7.5 g (81.4 mmol) of NBD and 0.525 g of surfactant (7 wt% in respect to NBD) were weighted. Subsequently, the mixture was stirred with a mechanical stirrer at 400rpm while 30 mL distilled water were added dropwise. After water addition, the mixture was turned into milky, gel-like emulsion and the stirring was continued for one more hour. 1.93 mg (0.002 mmol) of catalyst [1,3-Bis(2,4,6-trimethylpheny-l-2-imidazolidinylidene]dichloro(3-phenyl-1H-inden-1-ylidne)(trichloro-hexyl-phosphine) ruthenium(II) (M2) with molar ration of 1:40000 (regarding the NBD) was dissolved in 200 μL toluene and was added to the emulsion under agitation. The pinky mixture was poured into moulds and cured at 40 °C for 2h. The resulted white monoliths were placed in acetone for

10 min because they were oxidized quite fast in order to remove the surfactant. Finally, the samples were dried under vacuum at room temperature and stored under nitrogen for short period or under nitrogen in the fridge for longer period. Drying and storage under ambient conditions must be avoided due to the fast oxidation that can lead in some cases to combustion.

4.4.2 NBD HIPE stability studies

The emulsion stability of the NBD HIPEs prepared with different surfactants and DCPD HIPE was investigated with the optical microscopy (OM). The HIPEs were formulated according to 4.3.1 and 4.4.1, but without the addition of the catalyst and casted in two 20 mL vials. The first vial was kept at room temperature while the second was exposed at 40 °C, the typical polymerization temperature of NBD polymers. Immediately after the emulsion preparation and every 30 min for two hours, a small amount from the vials was taken, placed between two glasses in order to form a thin film and observed under the OM. The period of two hours was selected because they correspond to the standard polymerization duration for the NBD polyHIPEs. For every sample, a representative area was captured and evaluated. The diameter of at least 100 droplets was measured manually in order to give the mean value and the standard deviation, as well as the data distribution. Due to the pressure applied for the formation of the thin film, it was difficult to correctly evaluate the sizes. Consequently, droplets' diameters had to be multiplied with the correction factor $2/3^{1/2}$.

4.4.3 Oxygen measurements

Oxygen measurements on DCPD and NBD polyHIPEs were recorded by optical oxygen meter FireStingO_2 combined with a contactless oxygen sensor (sensor spot) from PyroScience. For NBD monoliths, two types of sensor with different oxygen sensing range were used, a normal sensor (reliable limits 1000hPa-1hPa) and a trace sensor (perfluoroalkylated Pt, Teflon AF 1600,[26] reliable limits 50hPa-0.003hPa). For DCPD monoliths only the normal sensor was used. The contactless sensors were spotted on a 250 mL schlenk flask, where the measurements were carried out (Figure 45). Prior to every measurement the calibration of the instrument was done for two points. One calibration point was under anoxic conditions (nitrogen) for both sensors, while the second point was under ambient conditions (air) for normal sensor and under 2 % O_2 for trace sensor. Additionally, the temperature, pressure and humidity indexes were necessary for the calibration. All measurements were carried out under atmospheric air which contains 20.95 % O_2.

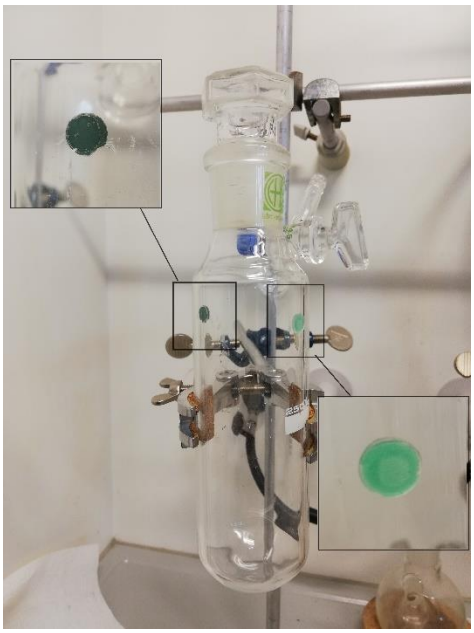

Figure 45. Sensor spots (normal sensor left, trace sensor right) spotted on the experimental flask.

The DCPD and NBD polyHIPEs were prepared according to 4.3.1 and 4.4.1 and casted in 20 mL vials, filling only the 1/5 of the vial. The big dry and unoxidized monoliths were firstly weighted and then placed into the schlenk flask. The flask was tightly sealed to prevent oxygen replacement from the surrounding environment, the air was pumped from the flask with vacuum and finally, the data collection started immediately after fresh air was inserted. The same procedure was carried out on samples pieces weighting 6 times less than the big monoliths. In order to take the small pieces, the big samples were carefully cut. Figure 46 shows the experimental setup of normal and trace sensor during a simultaneous measurement. Measurements performed on big NBD polyHIPEs required three flask refills for complete oxidation. In case of DCPD polyHIPEs and small NBD pieces, the flask was filled only once. Lastly, the samples were weighted after the measurement completion in order to indicate the mass increase and hence to evaluate the O_2 consumption.

Figure 46. Experimental setup during a simultaneous measurement of normal (left) and trace (right) sensors.

List of figures

List of tables

Bibliography

(1) Silverstein, M. S. PolyHIPEs: Recent Advances in Emulsion-Templated Porous Polymers. *Prog. Polym. Sci.* **2014**, *39* (1), 199–234.

(2) Wu, D.; Xu, F.; Sun, B.; Fu, R.; He, H.; Matyjaszewski, K. Design and Preparation of Porous Polymers. *Chem. Rev.* **2012**, *112* (7), 3959–4015.

(3) Silverstein, M. S., Cameron, N. R., Hillmyer, M. A.; Porous Polymers; John Wiley & Sons, Inc; **2011**.

(4) Pulko, I.; Krajnc, P. High Internal Phase Emulsion Templating--A Path to Hierarchically Porous Functional Polymers. *Macromol. Rapid Commun.* **2012**, *33* (20), 1731–1746.

(5) Cameron, N. R. High Internal Phase Emulsion Templating as a Route to Well-Defined Porous Polymers. *Polymer (Guildf).* **2005**, *46* (5), 1439–1449.

(6) Kovačič, S.; Krajnc, P.; Slugovc, C. Inherently Reactive PolyHIPE Material from Dicyclopentadiene. *Chem. Commun.* **2010**, *46* (40), 7504–7506.

(7) Kovacic, S.; Jeřábek, K.; Krajnc, P.; Slugovc, C. Ring Opening Metathesis Polymerisation of Emulsion Templated Dicyclopentadiene Giving Open Porous Materials with Excellent Mechanical Properties. *Polym. Chem.* **2012**, *3* (2), 325–328.

(8) Kovačič, S.; Matsko, N. B.; Jerabek, K.; Krajnc, P.; Slugovc, C. On the Mechanical Properties of HIPE Templated Macroporous Poly(Dicyclopentadiene) Prepared with Low Surfactant Amounts. *J. Mater. Chem. A* **2013**.

(9) Mert, E. H.; Slugovc, C.; Krajnc, P. Tailoring the Mechanical and Thermal Properties of Dicyclopentadiene PolyHIPEs with the Use of a Comonomer. *Express Polym. Lett.* **2015**.

(10) Kovačič, S.; Preishuber-Pflügl, F.; Slugovc, C. Macroporous Polyolefin Membranes from Dicyclopentadiene High Internal Phase Emulsions: Preparation and Morphology Tuning. *Macromol. Mater. Eng.* **2014**, *299* (7), 843–850.

(11) Knall, A. C.; Kovačič, S.; Hollauf, M.; Reishofer, D.; Saf, R.; Slugovc, C. Inverse Electron Demand Diels-Alder (IEDDA) Functionalisation of Macroporous Poly(Dicyclopentadiene) Foams. *Chem. Commun.* **2013**, *49* (66), 7325–7327.

(12) Kovačič, S.; Kren, H.; Krajnc, P.; Koller, S.; Slugovc, C. The Use of an Emulsion Templated Microcellular Poly(Dicyclopentadiene-Co- Norbornene) Membrane as a Separator in Lithium-Ion Batteries. *Macromol. Rapid Commun.* **2013**.

(13) Trupej, N.; Novak, Z.; Knez, Ž.; Slugovc, C.; Kovačič, S. Supercritical CO2mediated Functionalization of Highly Porous Emulsion-Derived Foams: ScCO2absorption and Epoxidation. *J. CO2 Util.* **2017**, *21* (July), 336–341.

(14) Kovačič, S.; Matsko, N. B.; Ferk, G.; Slugovc, C. Macroporous Poly(Dicyclopentadiene) Γfe2O3/Fe3O4nanocomposite Foams by High Internal Phase Emulsion Templating. *J. Mater. Chem. A* **2013**, *1* (27), 7971–7978.

(15) Kovačič, S.; Matsko, N. B.; Ferk, G.; Slugovc, C. Nanocomposite Foams from Iron Oxide

Stabilized Dicyclopentadiene High Internal Phase Emulsions: Preparation and Bromination. *Acta Chim. Slov.* **2014**, *61* (1), 208–214.

(16) Kovačič, S.; Anžlovar, A.; Erjavec, B.; Kapun, G.; Matsko, N. B.; Žigon, M.; Žagar, E.; Pintar, A.; Slugovc, C. Macroporous ZnO Foams by High Internal Phase Emulsion Technique: Synthesis and Catalytic Activity. *ACS Appl. Mater. Interfaces* **2014**, *6* (21), 19075–19081.

(17) Kovacic, S.; Mazaj, M.; Jeselnik, M.; Pahovnik, D.; Zagar, E.; Slugovc, C.; Logar, N. Z. Synthesis and Catalytic Performance of Hierarchically Porous MIL-100(Fe)@polyHIPE Hybrid Membranes. *Macromol Rapid Commun* **2015**, *36* (17), 1605–1611.

(18) Williams, J. M.; Gray, A. J.; Wilkerson, M. H. Emulsion Stability and Rigid Foams from Styrene or Divinylbenzene Water-in-Oil Emulsions. *Langmuir* **1990**, *6* (2), 437–444.

(19) Kovačič, S.; Preishuber-Pflügl, F.; Pahovnik, D.; Žagar, E.; Slugovc, C. Covalent Incorporation of the Surfactant into High Internal Phase Emulsion Templated Polymeric Foams. *Chem. Commun.* **2015**, *51* (36), 7725–7728.

(20) Tire, T. F.; Company, R. The Infrared Spectra and Structures of Poly but Adienes *. **2000**, *1* (June 1961), 47–58.

(21) Kerry, J., Butler, P.; Smart Packaging Technologies for Fast Smart Packaging Technologies for Fast Moving; John Wiley & Sons, Ltd; **2008**.

(22) Chu, C.; Lin, K.; Tang, Y. Sensors and Actuators B : Chemical A New Optical Sensor for Sensing Oxygen Based on Phase Shift Detection. *Sensors Actuators B. Chem.* **2016**, *223*, 606–612.

(23) Bauman, R. G.; Maron, S. H. Oxidation of Polybutadiene . I . Rate of Oxidation. *J. Polym. Sci.* **1956**, *XXII*, 1–12.

(24) Riddick, J.A.; Bunger, W.B.; Sakano, T.K. *Organic solvents: physical properties and methods of purification.* Fourth edition; Wiley-Interscience: New York, **1986**.

(25) Idris, N. H.; Rahman, M. M.; Wang, J. Z.; Liu, H. K. Microporous Gel Polymer Electrolytes for Lithium Rechargeable Battery Application. *J. Power Sources* **2012**, *201*, 294–300.

(26) Larsen, M.; Lehner, P.; Borisov S. M.; Klimant, I.; Fischer, J. P.; Stewart, F. J.; Canfield, D. E.; Glud, R. N. In situ quantification of ultra-low O_2 concentrations in oxygen minimum zones: Application of novel optodes. *Limnol. Oceanogr.: Methods* **2016**, *14*: 784–800.

Appendix A Molecular structure of surfactants

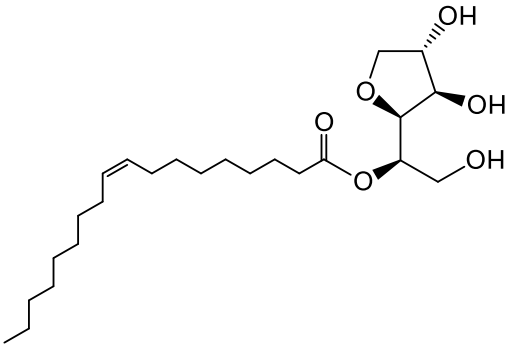

Figure A1. Molecular structure of surfactant Sorbitan monooleate (Span80)

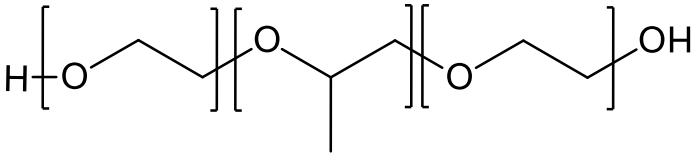

Figure A2. Molecular structure of surfactants Pluronic L-121 and P-123

Appendix B Experimental Results

Tables A1-A5 have been resulted according to 4.3.3 procedure.

Table A1. Weights, dimensions and observations for the polymerization of P0 for 2, 3, 4, 5, 6, 7 and 24h at 80 °C.

P0	***2h***	***3h***	***4h***	***5h***	***6h***	***7h***	***24h***
Emulsion (before curing) (g)	1.5942	1.6211	1.6071	1.6925	1.6078	1.5916	1.6362
Wet foams (after curing) (g)	1.4469	1.44	1.4399	1.4077	1.4215	1.4117	1.2165
Cured/uncured difference (%)	9.24	11.17	10.40	16.83	11.59	11.30	25.65
Dry foams (g)	0.2876	0.2780	0.2754	0,2798	0,2788	0,2797	0.2953
Wet/dry difference (%)	80.12	80.69	80.87	80.12	80.39	80.19	75.73
thickness (mm)	2.010	1.995	2.000	2.000	2.010	1.990	-
diameter (mm)	29.797	29.677	29.712	29.505	29.552	29.790	-
Observations	unox	unox	unox	ox edges	ox edges	ox edges	ox

Table A2. Weights, dimensions and observations for the polymerization of P10 for 2, 3, 4, 5, 6, 7 and 24h at 80 °C.

P10	***2h***	***3h***	***4h***	***5h***	***6h***	***7h***	***24h***
Emulsion (before curing) (g)	1.6167	1.5519	1.5741	1,5855	1,5548	1.6018	1.5992
Wet foams (after curing) (g)	1.4673	1.4514	1.4503	1.4179	1.4415	1.4056	1.304
Cured/uncured difference (%)	9.24	6.48	7.86	10.57	7.29	12.25	18.46
Dry foams (g)	0.3115	0.2928	0.3094	0.2912	0.3000	0.3148	0.3171
Wet/dry difference (%)	78.77	79.83	78.67	79.46	79.19	77.60	75.68
thickness (mm)	2.017	1.990	1.987	2.010	1.990	1.998	-
diameter (mm)	29.692	29.517	29.602	29.415	29.630	29.793	-
Observations	unox	unox	unox	ox edges	ox edges	ox edges	ox

Table A3. Weights, dimensions and observations for the polymerization of P40 for 2, 3, 4, 5, 6, 7 and 24h at 80 °C.

P40	***2h***	***3h***	***4h***	***5h***	***6h***	***7h***	***24h***
Emulsion (before curing) (g)	1.5786	1.5592	1.5734	1.5591	1.5657	1.3162	1.6567
Wet foams (after curing) (g)	1.4725	1.4586	1.4592	1.449	1.4392	1.1181	1.2399
Cured/uncured difference (%)	6.72	6.45	7.26	7.06	8.08	15.05	25.16
Dry foams (g)	0.2963	0.3035	0.3049	0.3173	0.3131	0.3207	0.3213
Wet/dry difference (%)	79.88	79.19	79.10	78.10	78.24	71.32	74.09
thickness (mm)	2.010	2.000	2.010	2.005	2,020	2.040	-
diameter (mm)	29.650	29.783	29.723	29.822	29.770	29.990	-
Observations	unox	unox	unox	unox	unox	ox edges	ox

Table A4. Weights, dimensions and observations for the polymerization of P20 for 2, 3, 4, 5, 6, 7 and 24h at 80 °C.

P20	***2h***	***3h***	***4h***
Emulsion (before curing) (g)	1.5434	1.5787	1.6499
Wet foams (after curing) (g)	1.4666	1.4557	1.4488
Cured/uncured difference (%)	4.98	7.79	12.19
Dry foams (g)	0.2947	0.3081	0.31
Wet/dry difference (%)	79.9	78.8	78.6
thickness (mm)	2.010	2.040	2.027
diameter (mm)	29.732	29.61	29.817
Observations	unox	unox	unox

Table A5. Weights, dimensions and observations for the polymerization of P30 for 2, 3, 4, 5, 6, 7 and 24h at 80 °C.

P30	***2h***	***3h***	***4h***
Emulsion (before curing) (g)	1.6070	1.6010	1.5052
Wet foams (after curing) (g)	1.4899	1.4827	1.4084
Cured/uncured difference (%)	7.29	7.39	6.43
Dry foams (g)	0.3457	0.3490	0.3254
Wet/dry difference (%)	76.8	76.5	76.9
thickness (mm)	1.992	1.995	2.002
diameter (mm)	29.630	29.725	29.727

Observations	unox	unox	unox

Tables A6 has been resulted according to 4.3.5 procedure.

Table A6. Porosity results after immersion in water and ethanol.

Porosity (%)	***Water***	***Ethanol***
P0	71.3 ± 2.8	81.7 ± 1.0
P10	77.0 ± 1.2	82.8 ± 0.6
P20	79.4 ± 0.5	82.7 ± 0.3
P30	78.3 ± 0.9	83.2 ± 0.6
P40	76.8 ± 2.0	85.4 ± 0.9

Tables A7 has been resulted according to 4.3.54.3.5 procedure assuming that the porosity is 80% for all cases.

Table A7. Calculated density by the immersion results in water and ethanol.

Density (g/L)	***Water***	***Ethanol***
P0	1.081	1.067
P10	1.068	1.082
P20	1.091	1.094
P30	1.084	1.099
P40	1.089	1.100

Table A8. Voids and windows mean diameter of DCPD/CLC polyHIPE samples.

DCPD/CLC	***Voids***	***Windows***
P0	5.95 ± 2.05	1.16 ± 0.42
P10	6.67 ± 3.55	1.29 ± 0.67

P20	7.95 ± 3.39	1.36 ± 0.81
P30	7.48 ± 1.86	1.17 ± 0.56
P40	6.98 ± 1.96	1.18 ± 0.61

Table A9. Voids and windows mean diameter of NBD polyHIPE samples.

NBD	***Voids***	***Windows***
L-121	15.19 ± 8.28	4.05 ± 2.13
Span80	12.61 ± 5.98	2.58 ± 0.87

Table A10. Droplets mean size of NBD/Span80 polyHIPE sample.

Time (min)	***NBD/Span80 (r.t.)***	***NBD/Span80 (40 °C)***
0	12.70 ± 5.03	12.70 ± 5.03
30	12.65 ± 4.11	12.81 ± 3.74
60	14.83 ± 4.63	14.03 ± 4.43
90	12.72 ± 4.53	15.79 ± 5.06
120	13.45 ± 3.23	15.81 ± 5.04

Table A11. Droplets mean size of NBD/L-121 polyHIPE sample.

Time (min)	***NBD/L-121 (r.t.)***	***NBD/L-121 (40 °C)***
0	17.70 ± 6.29	17.70 ± 6.29
30	19.63 ± 6.82	19.84 ± 7.86
60	19.16 ± 8.32	22.03 ± 9.46
90	17.56 ± 7.93	22.09 ± 10.21
120	19.63 ± 8.78	separation

Table A12. Droplets mean size of NBD/P-123 polyHIPE sample.

Time (min)	***NBD/P123 (r.t.)***	***NBD/P123 (40 °C)***
0	7.99 ± 1.91	7.99 ± 1.91
30	7.98 ± 1.78	8.10 ± 2.05

60	8.39 ± 2.37	separation
90	8.61 ± 2.15	separation
120	separation	separation

Table A13. Droplets mean size of DCPD/L-121 polyHIPE sample.

Time (min)	***DCPD/L-121 (r.t.)***	***DCPD/L-121 (40 °C)***
0	9.78 ± 2.70	9.78 ± 2.70
30	9.36 ± 1.99	9.34 ± 2.50
60	10.61 ± 3.21	10.39 ± 2.96
90	9.96 ± 2.62	9.45 ± 2.83
120	10.95 ± 2.48	10.15 ± 2.82

Tables A14-A16 has been resulted according to 4.3.4 procedure.

Table A14.Swelling results of P0, P10, P20, P30 and P40 after immersion in water, ethanol, n-pentanol, acetone and toluene

Swelling (volume %)	***Water***	***Ethanol***	***n-Pentanol***	***Acetone***	***Toluene***
P0	0.24 ± 0.17	0.69 ± 0.05	4.03 ± 0.30	3.74 ± 0.15	62.59 ± 2.27
P10	0.23 ± 0.03	1.36 ± 0.59	5.90 ± 0.12	5.07 ± 0.27	41.40 ± 0.24
P20	1.32 ± 0.25	2.04 ± 0.25	6.33 ± 1.28	5.20 ± 0.98	42.16 ± 0.33
P30	0.55 ± 0.34	1.26 ± 0.48	6.35 ± 0.65	6.94 ± 0.63	36.05 ± 4.11
P40	1.87 ± 0.08	3.15 ± 0.38	6.77 ± 0.22	8.11 ± 0.25	30.44 ± 1.54

Table A15. Deswelling results of P0, P10, P20, P30 and P40 after immersion in water, ethanol, n-pentanol, acetone and toluene

Deswelling (volume %)	***Water***	***Ethanol***	***n-Pentanol***	***Acetone***	***Toluene***
P0	-2.95 ± 0.00	-6.78 ± 0.79	-3.51 ± 2.17	-7.98 ± 0.34	-220.47 ± 2.37
P10	-2.38 ± 1.10	-7.15 ± 0.82	-4.04 ± 0.67	-7.24 ± 0.00	-9.07 ± 6.27
P20	-1.33 ± 0.33	-4.21 ± 0.79	-3.55 ± 0.42	-3.97 ± 1.47	-6.90 ± 3.76
P30	-1.47 ± 0.84	-5.40 ± 1.50	-4.13 ± 1.13	-6.55 ± 1.23	0.40 ± 1.36
P40	-1.24 ± 0.00	-3.22 ± 0.85	-2.06 ± 1.07	-6.76 ± 1.07	3.20 ± 4.18

Table A16. Solvent uptake results of P0, P10, P20, P30 and P40 after immersion in water, ethanol, n-pentanol, acetone and toluene

Solvent uptake (wt%)	***Water***	***Ethanol***	***n-Pentanol***	***Acetone***	***Toluene***
P0	334.4 ± 14.2	298.3 ± 5.5	319.1 ± 1.2	301.3 ± 1.6	1147.8 ± 18.5
P10	363.9 ± 12.2	310.3 ± 5.5	325.3 ± 9.2	309.8 ± 7.7	726.9 ± 16.2
P20	362.9 ± 3.1	299.0 ± 4.4	323.5 ± 5.5	302.9 ± 7.3	650.3 ± 10.7
P30	356.1 ± 5.0	302.9 ± 0.5	323.8 ± 1.5	314.1 ± 1.0	564.3 ± 22.5
P40	348.7 ± 5.3	309.4 ± 5.7	311.8 ± 5.8	313.3 ± 0.2	555.9 ± 16.3

Table A 17. Tensile test results for P0, P10, P20, P30 and P40 extracted by stress-strain curve.

DCPD/CLC	***P0***	***P10***	***P20***	***P30***	***P40***
Young's modulus (MPa)	103 ± 3	106 ± 5	114 ± 5	115 ± 2	117 ± 3
Ultimate tensile strength (MPa)	2.65 ± 0.12	2.18 ± 0.21	2.72 ± 0.24	2.51 ± 0.18	2.61 ± 0.13
max strain (%)	42.0 ± 3.5	23.8 ± 4.6	17.1 ± 1.3	9.2 ± 2.0	8.0 ± 1.5
Modulus of toughness (MJ/m^3)	0.84 ± 0.07	0.39 ± 0.10	0.36 ± 0.03	0.19 ± 0.06	0.16 ± 0.04
0.2 % offset yield point (MPa)	1.00 ± 0.16	0.80 ± 0.08	1.44 ± 0.20	1.64 ± 0.15	1.67 ± 0.04
0.2 % offset yield point (%)	0.012 ± 0.002	0.009 ± 0.001	0.015 ± 0.002	0.017 ± 0.001	0.017 ± 0.001
Modulus of resilience (MJ/m^3)	0.007 ± 0.002	0.004 ± 0.001	0.012 ± 0.003	0.016 ± 0.003	0.016 ± 0.001

Table A18. Tensile test results for P0, P10, P20, P30 and P40 extracted by stress-strain curve.

NBD	***NBD/Span80***	***NBD/L-121***
Young's modulus (MPa)	48 ± 8	68 ± 9
Ultimate tensile strength (MPa)	0.62 ± 0.11	1.07 ± 0.03
max strain (%)	47 ± 12	105 ± 11
Modulus of toughness (MJ/m^3)	0.25 ± 0.05	0.86 ± 0.08
0.2 % offset yield point (MPa)	0.30 ± 0.09	0.45 ± 0.08
0.2 % offset yield point (%)	0.009 ± 0.001	0.008 ± 0.001
Modulus of resilience (MJ/m^3)	0.0016 ± 0.0007	0.006 ± 0.002

Appendix C Additional graphs

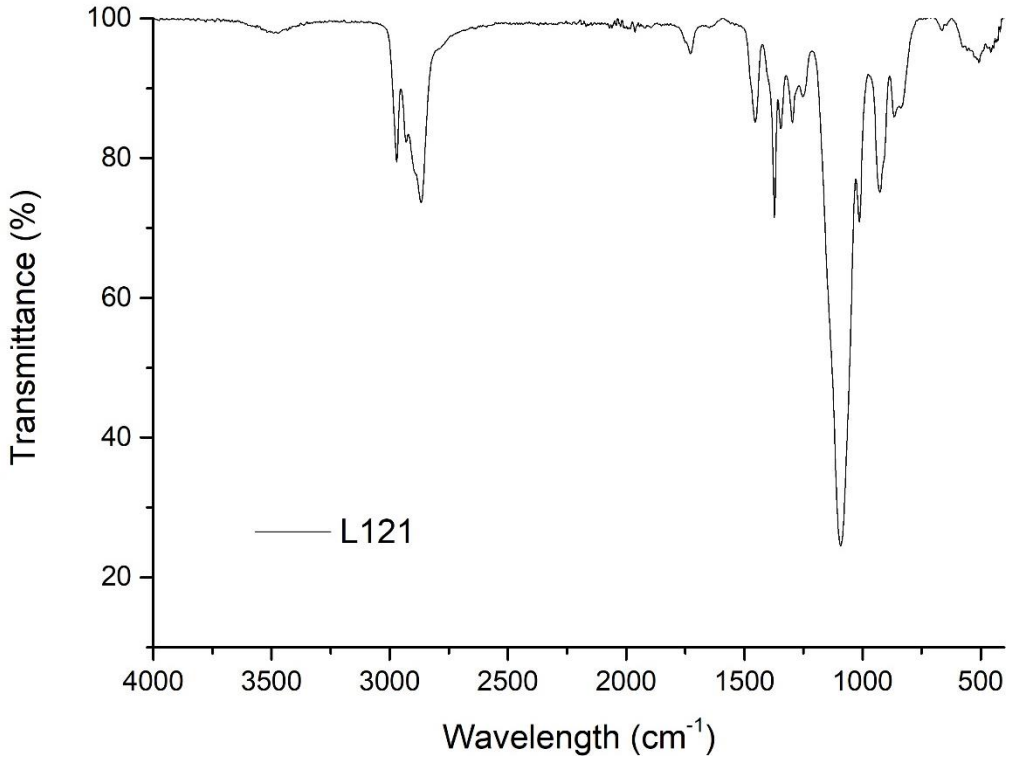

Figure A3. IR spectrum of surfactant L-121

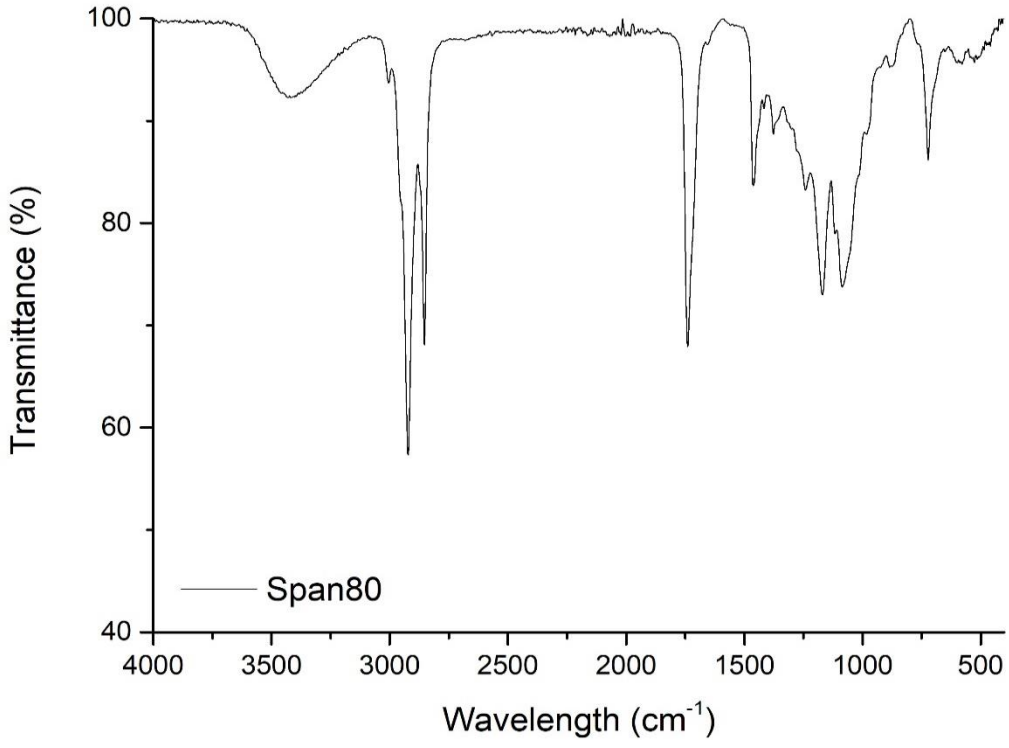

Figure A4. IR spectrum of surfactant Span80.

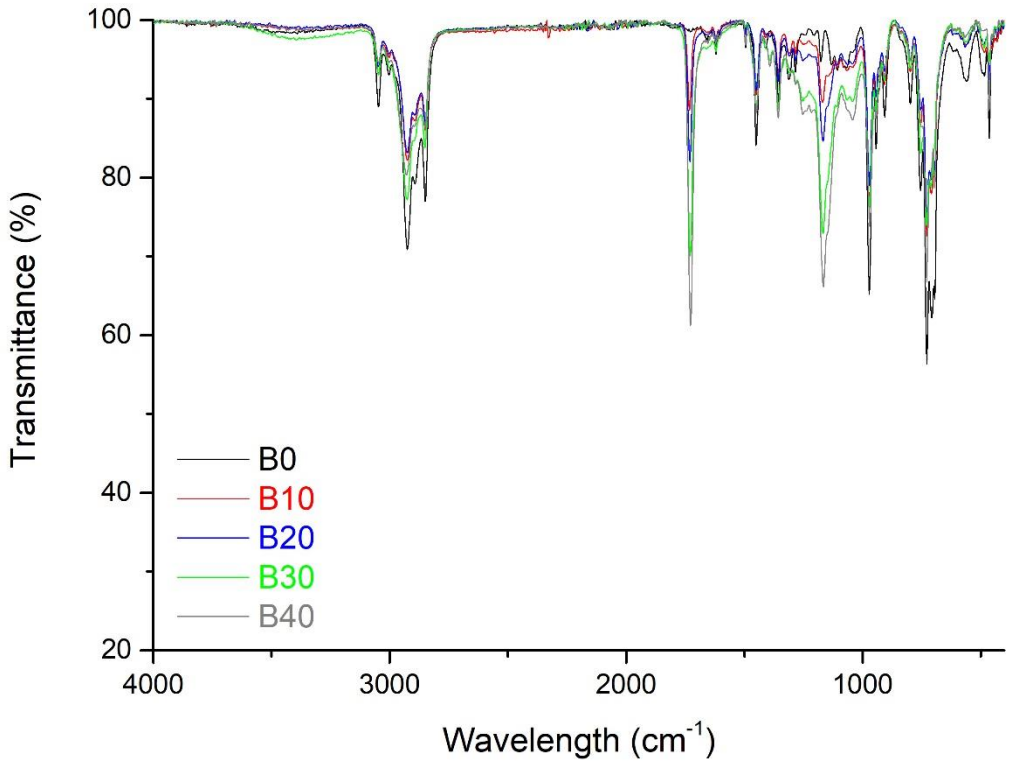

Figure A5. IR spectra of bulk copolymers.

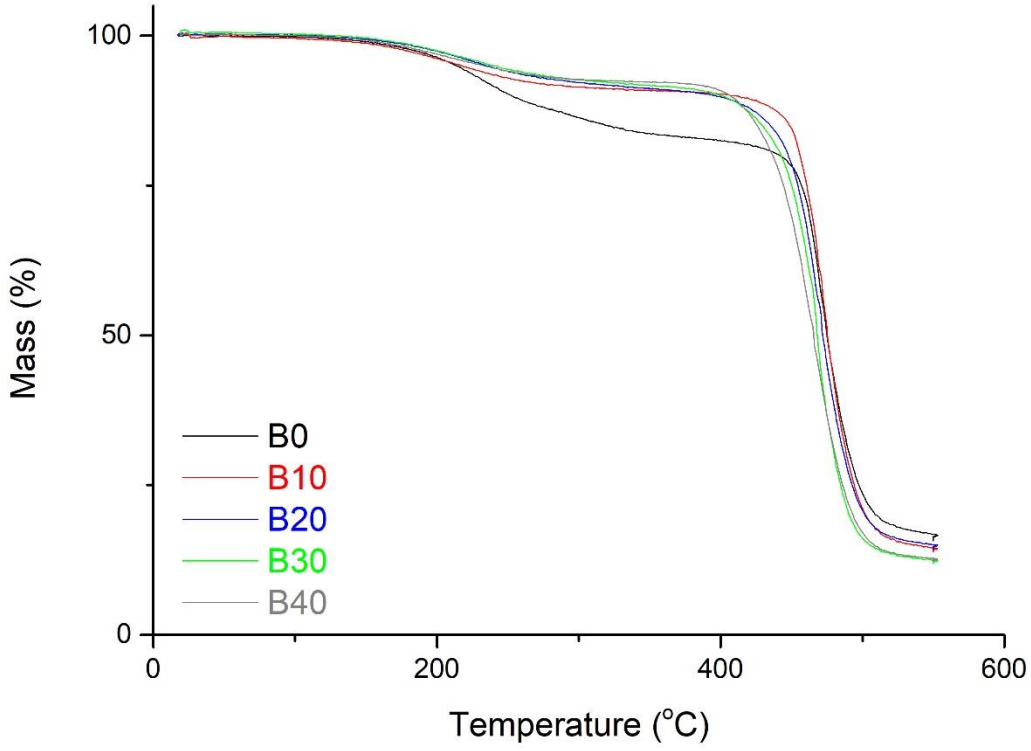

Figure A6. TGA curves of bulk copolymers

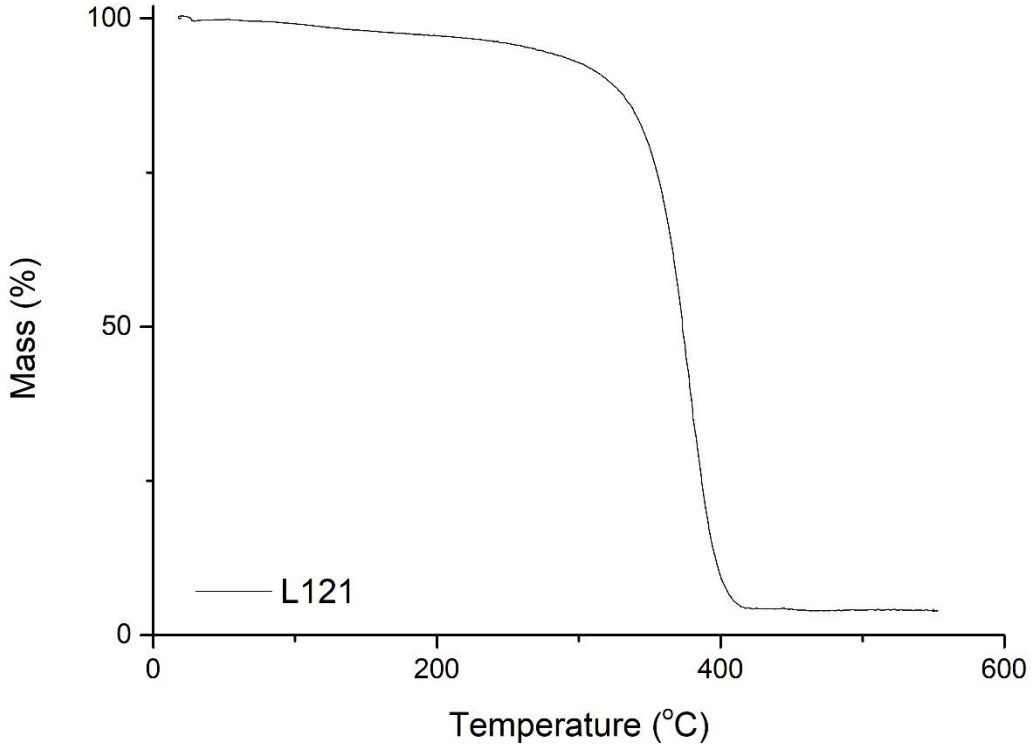

Figure A7. TGA curves of surfactant L-121.

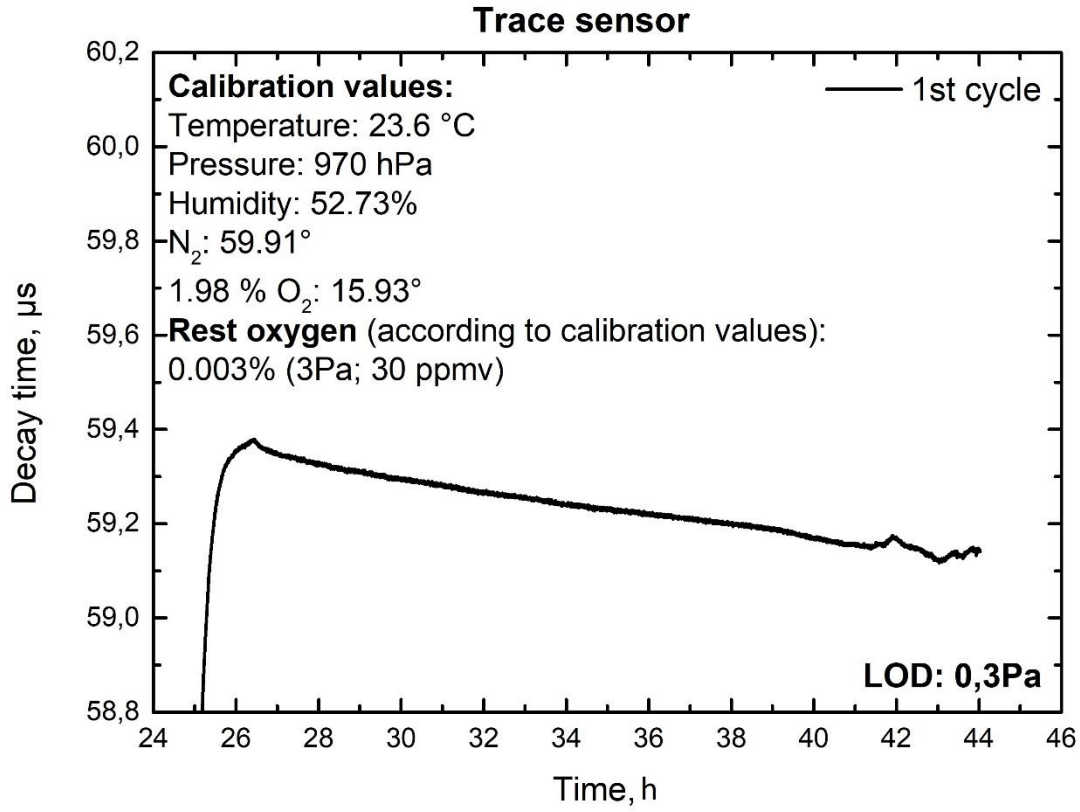

Figure A8. Oxygen measurements recorded by trace sensor on big NBD polyHIPE (1st flask fill).

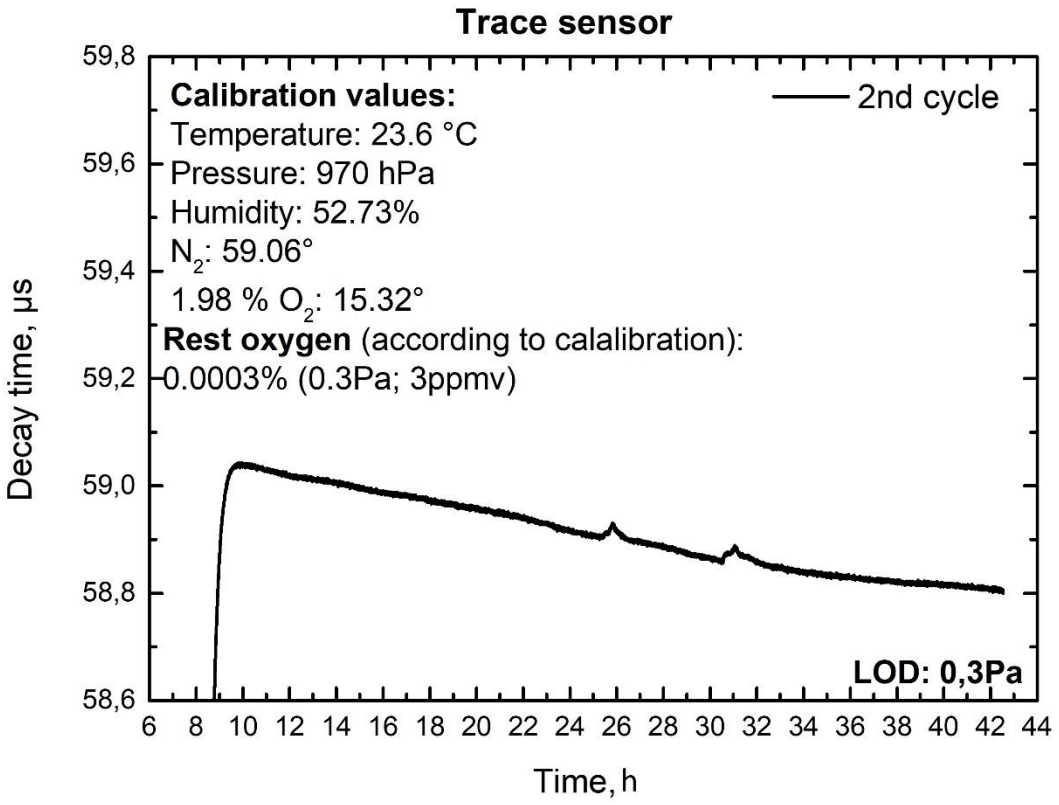

Figure A9. Oxygen measurements recorded by trace sensor on big NBD polyHIPE (2nd flask fill).